

Advanced Laboratory in Mechanical Engineering (034057)

Lab 2: Vibrations

05/06/2023

Lab Instructor: Aharon Levin



Due date: 24.06.2024

E-mail	ID	Name
dannyapsel@campus.technion.ac.il	[REDACTED]	Danny Apsel
[REDACTED]	[REDACTED]	[REDACTED]

We did not receive any consultation/discussion with members of other groups or with students who took the course in the past. We did not use a report/project that was written in previous semesters (reference). We did not use a tool based on artificial intelligence such as Chat GPT

Table of Contents

.1	Introduction	3
1.1	Experimental setup.....	3
1.2	Lab objectives	4
2.	Sensor Calibration:	7
3.	Sampling Experiment	10
3.1	11 [Hz] sampling experiment	11
3.2	27 [Hz] sampling experiment	13
3.3	33 [Hz] sampling experiment	15
3.4	60 [Hz] sampling experiment	17
3.5	1000 [Hz] sampling experiment.....	19
3.6	Sampling experiment Summary.....	21
4.	Linearity verification	22
5.	Natural Frequencies using Step response	25
6.	Eigenvector analysis.....	28
7.	Summary.....	35

1. Introduction

1.1 Experimental setup

Figure 1 shows an image of the experimental setup, which consists of flexible elements, including straight and arched spring elements, connecting rigid metal blocks (masses) to form a structure where there is a mutual influence between the different masses, springs, and the excitation system. Moving one mass causes the other masses to move due to forces exerted by the flexible elements. Dynamic forces in the x-direction can be applied via an electromagnetic actuator (voice coil).

The experimental system includes several additional components. Laser-based optical sensors, where the laser beam is tilted by the movement of each mass, and electronic sensors produce a voltage correlated to the relative position of one of the masses in the x-direction. There is a micrometric system that allows control of the magnet distance from the mass surface, creating forces opposite to the relative velocity between masses and the magnet, which act as damping forces on each mass separately. An electronic card controlled by a computer, using MATLAB during the experiment, converts the four sensor voltages into vectors that can be translated into equivalent engineering sizes (displacement in [mm]) through a process called sampling. Additionally, an electrical signal can be generated for actuating the voice coil, and the current passing through the electromagnet coil can be measured. The actuator force is proportional to the current and can be calibrated.



Figure 1: Experimental setup

1.2 Lab objectives

The primary objective of this laboratory is to learn and practice methods for characterizing vibrating systems and identifying system characteristics such as natural frequencies, modes of vibration (eigenvectors), and damping coefficients. This includes familiarization with the Stepped Sine Testing measurement method. Additionally, the lab aims to teach and practice methods for analysing measured vibrating signals, particularly using FFT (Fast Fourier Transform) and fitting non-linear functions to experimental results. It also seeks to illustrate principles and concepts from vibration theory, specifically the principle of superposition in linear systems, Bode plots, and concepts such as the Q-Factor. Furthermore, the lab aims to familiarize participants with calibration procedures and to understand and use measurement equipment, recognizing how the specifications of the equipment affect the accuracy of the experiment. This includes the impact of the resolution and accuracy of the PSD sensor, the effect of sampling frequency, and the influence of the signal-to-noise ratio on the values extracted from the experiment.

Experiment 1: Sensor Calibration

Each group begins by calibrating the sensors and saving the calibration curves for the final report according to the instructions provided in the calibration section in the pre-lab report, utilizing the *SensorCalibration.m* file. This step ensures that all measurements taken during the experiments are accurate and reliable.

Experiment 2: Sampling experiment

The next step involves enabling a 15 [Hz] sine actuation and sampling the signals at the following frequencies: 11 [Hz], 27 [Hz], 33 [Hz], 60 [Hz] and 1000 [Hz]. The data is saved using the *SinInputDownSampled.m* file. This experiment aims to measure the system's frequency response and generate the frequencies of every mass by using both FFT (Fast Fourier Transform) and LS (Least Squares) procedures.

Experiment 3: Linearity Test

The system's linearity is verified using the *LinearityTest.m* and *LinearityScript.m* files. Two sinusoidal signals with different frequencies are applied. Then, an input signal equal to the linear composition of the two sinusoidal signals is applied. The difference between the combination of the two sinusoidal signals and the linear composition inputs signal is calculated. This step ensures that the system behaves linearly within the tested range, validating the applicability of linear vibration theory to the system.

Experiment 4: Natural Frequencies using Step response

The response of the 4 masses with a step response input is analyzed using the *SquareInput.m* file. The natural frequencies of the system are calculated using the *Calc_fourier_from_data.m* file. This experiment provides an understanding of the system's dynamic response to a sudden excitation.

Experiment 5: Eigenvector analysis

Next, a sinusoidal excitation profile is applied using the *SinInput.m* file at each of the resonance frequencies found in the previous section. The program records the signals from the four sensors and the current in the actuator. By examining the MATLAB screen, the phase (0 or 180 degrees) between the signals of the four sensors at each of the resonant frequencies is estimated. This experiment helps in understanding the phase relationships and the modal behavior of the system at resonance.

2. Sensor Calibration:

We will use a known input signal to stimulate the first mass, activating the system. The positions of the four masses were measured using an external sensor. The calibration curves for each of the 4 masses can be seen below.

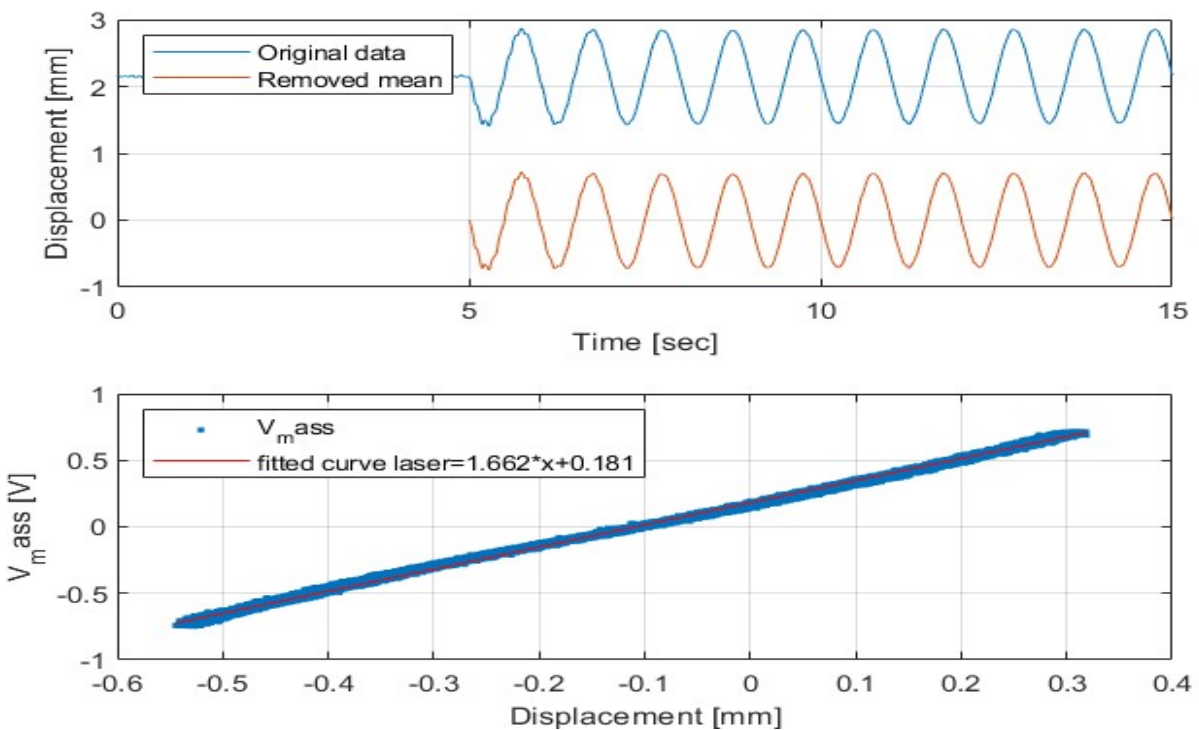


Figure 2: Sensor Calibration for Mass 1

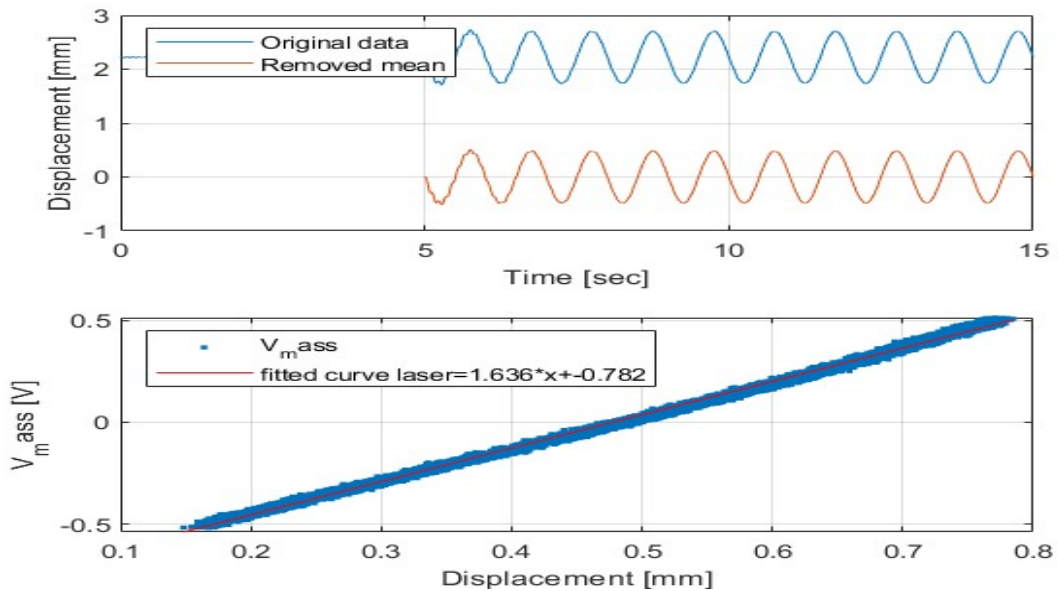


Figure 3: Sensor Calibration for Mass 2

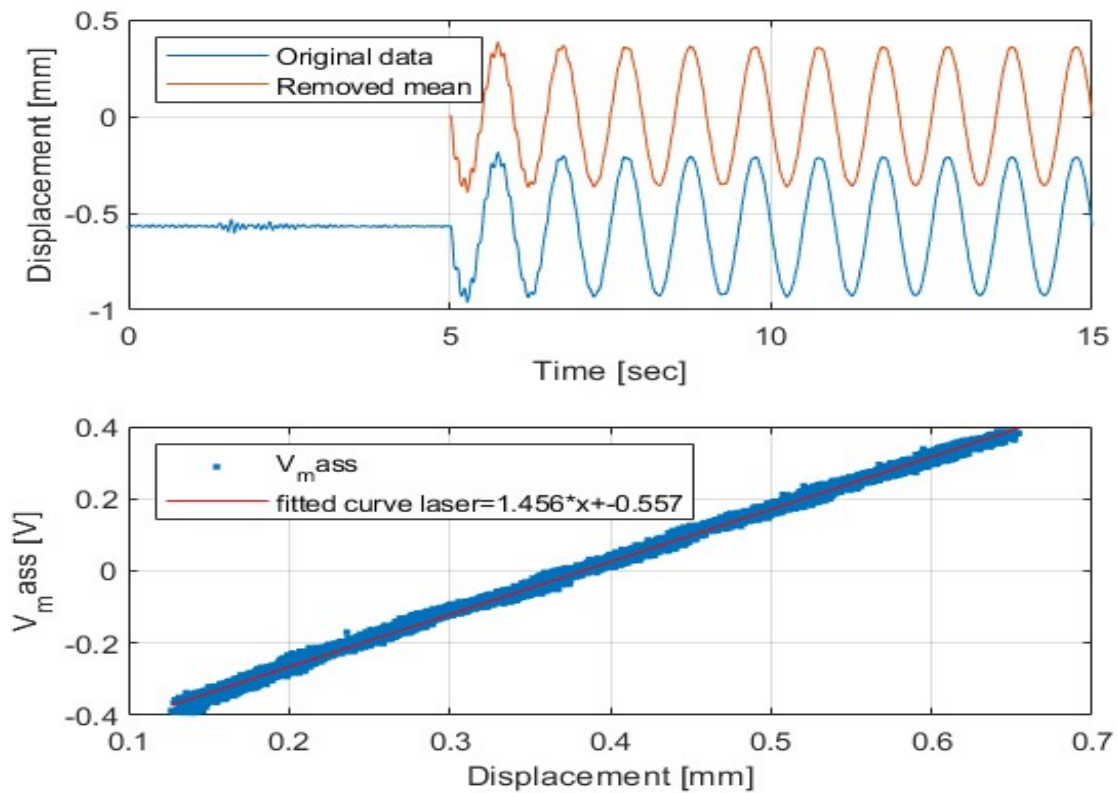


Figure 4: Sensor Calibration for Mass 3

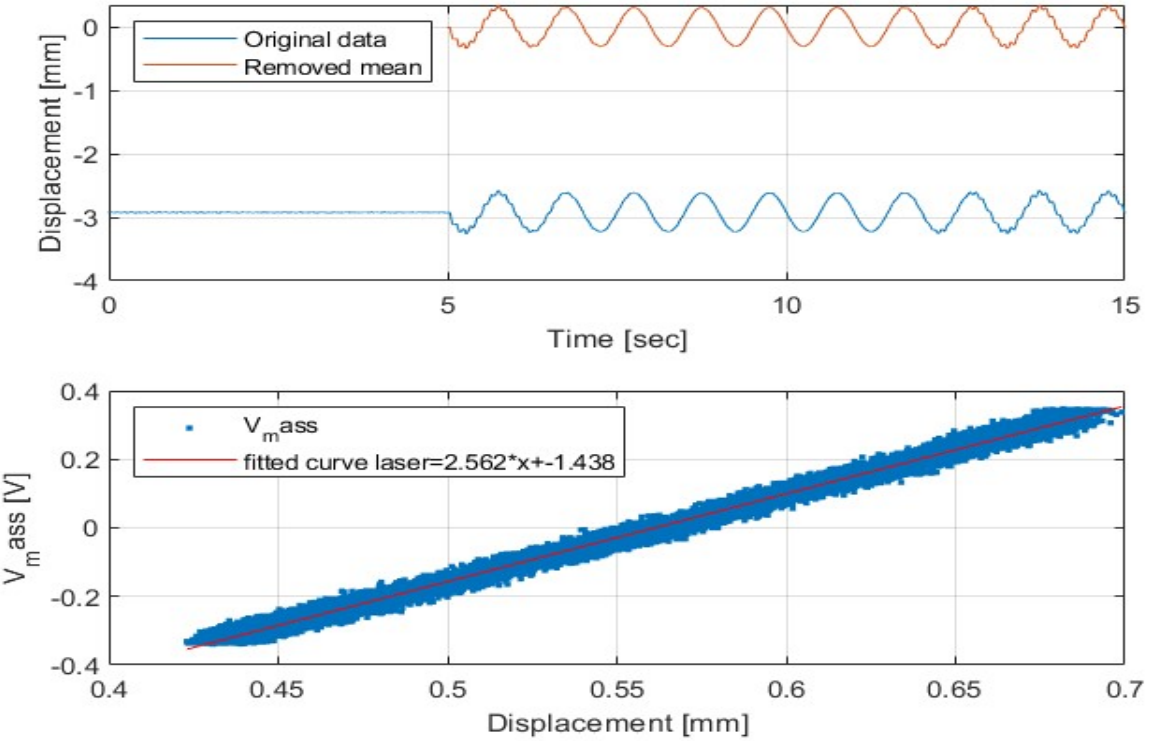


Figure 5: Sensor Calibration for Mass 4

Mass	Equation	R ²
1	1.662x + 0.181	0.999
2	1.636x - 0.782	0.998
3	1.456x - 0.557	0.999
4	2.562x - 1.438	0.996

Table 1: Linear Regression of Sensor Calibration

We can see that all 4 masses have a linear curve between the calibration sensor and the constant experiment sensors, with a very high accuracy.

3. Sampling Experiment

In this experiment, we excited the system with a sine wave at a frequency of 15 [Hz] and sampled the response at frequencies of 11 [Hz], 27 [Hz], 33 [Hz], 60 [Hz] and 1000 [Hz]. The number of samples obtained in a single sine cycle is determined by the ratio between the sampling frequency and the system frequency. Therefore, we can summarize the number of samples for different frequencies per cycle:

$$\left\{ \begin{array}{l} 11 \text{ [Hz]} \rightarrow \text{below 1 sample per cycle} \\ 27 \text{ [Hz]} \rightarrow \text{between 1 and 2 samples per cycle} \\ 33 \text{ [Hz]} \rightarrow \text{between 2 and 3 samples per cycle} \\ 60 \text{ [Hz]} \rightarrow \text{exactly 4 samples per cycle} \\ 1000 \text{ [Hz]} \rightarrow \text{between 66 and 67 samples per cycle} \end{array} \right.$$

According to the Nyquist-Shannon sampling theorem, when an analog signal is sampled at a frequency f , the sampled signal can be accurately reconstructed for frequencies up to $\frac{f}{2}$. If the sampled signal contains frequencies higher than this threshold, aliasing occurs, causing high-frequency information to appear at lower frequencies.

In this experiment, we anticipate that sampling frequencies below 30 Hz will result in aliasing. Sampling frequencies of 33 Hz, 60 Hz, and 1000 Hz will reliably represent the sampled signal without aliasing.

The sampling process demonstrates how the accuracy of the reconstructed signal depends on the sampling frequency relative to the original signal frequency, highlighting the importance of meeting the Nyquist criterion to avoid aliasing effects.

3.1 11 [Hz] sampling experiment

The Fourier transformation for 11 [Hz] can be seen below.

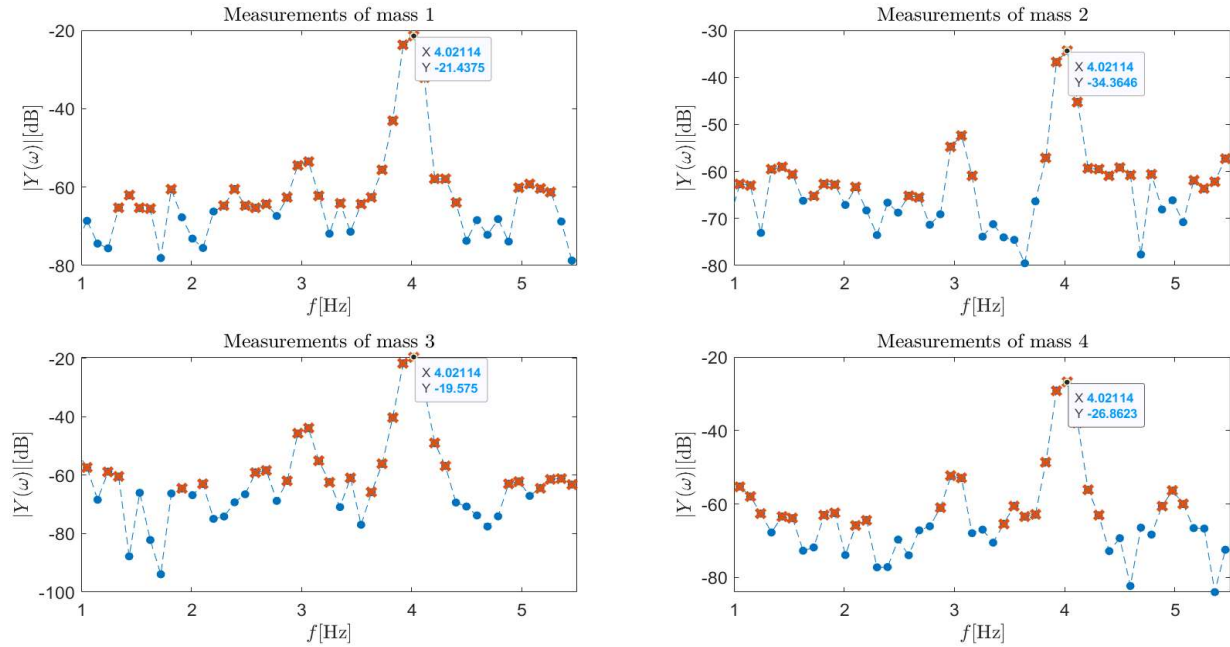


Figure 6: Fourier transformation for $f_s = 11$ [Hz]

We can obtain the amplitude $M = 10^{M_{Db}/20}$. The frequency f [Hz] of the response $y_n = 2M * \sin(2\pi ft)$ is shown in Figure 6.

Mass	2^*M [V]	M [V]	f [Hz]
1	$10^{-\frac{21.4375}{20}} = 0.0847$	0.04235	4.0211
2	$10^{-\frac{-34.3646}{20}} = 0.01913$	0.009565	4.0211
3	$10^{-\frac{-19.575}{20}} = 0.105$	0.0525	4.0211
4	$10^{-\frac{-26.8623}{20}} = 0.0454$	0.0227	4.0211

Table 2: Fourier transformation results for $f_s = 11$ [Hz]

We will now fit our response to the curve $y_n = M * \sin(2\pi f t + \phi) + D$ using the LS method, where M , ϕ and D are the parameters we'd like to find. This was done using MATLAB's Cftool. The results can be seen in Table 3.

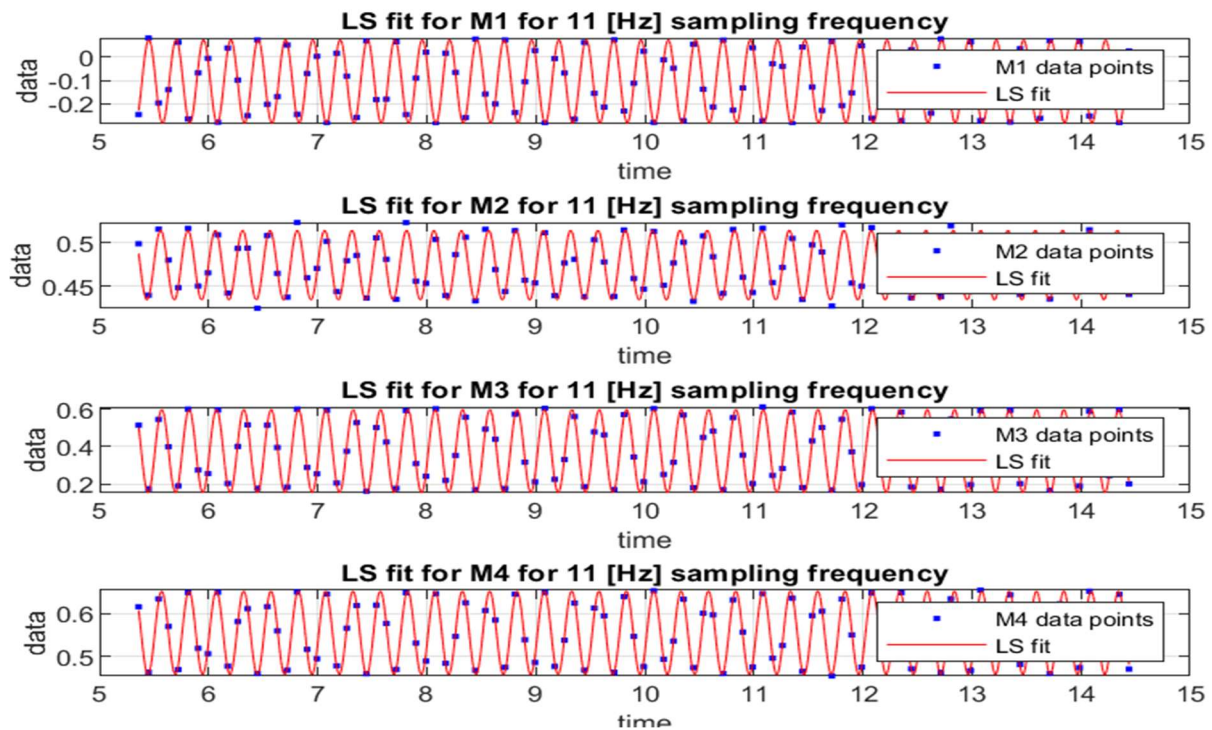


Figure 7: LS fit for $f_s = 11$ [Hz]

Mass	M	f [Hz]	ϕ [rad]	D	R²
1	-0.1794	3.989	0.01457	-0.105	0.996
2	0.03973	3.989	0.4482	0.4744	0.9521
3	0.2226	3.989	0.1776	0.3757	0.9935
4	0.09623	3.989	0.212	0.5552	0.9891

Table 3: LS fit results for $f_s = 11$ [Hz]

3.2 27 [Hz] sampling experiment

The Fourier transformation for 27 [Hz] can be seen below.

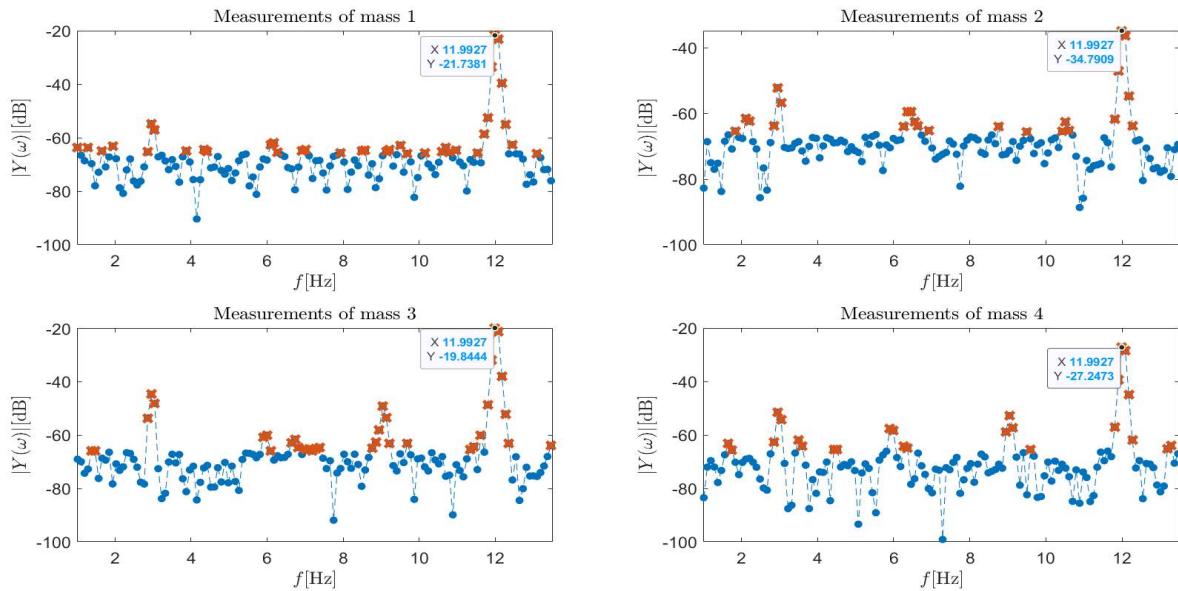


Figure 8: Fourier transformation for $f_s = 27$ [Hz]

We can obtain the amplitude $M = 10^{M_{Db}/20}$. The frequency f [Hz] of the response $y_n = 2M * \sin(2\pi ft)$ is shown in Figure 8.

Mass	2^*M [V]	M [V]	f [Hz]
1	$10^{-\frac{21.7381}{20}} = 0.08186$	0.04093	11.9927
2	$10^{-\frac{-34.7909}{20}} = 0.01822$	0.00911	11.9927
3	$10^{-\frac{-19.8444}{20}} = 0.1018$	0.0509	11.9927
4	$10^{-\frac{-27.2473}{20}} = 0.0434$	0.0217	11.9927

Table 4: Fourier transformation results for $f_s = 27$ [Hz]

We will now fit our response to the curve $y_n = M * \sin(2\pi f t + \phi) + D$ using the LS method, where M , ϕ and D are the parameters we'd like to find. This was done using MATLAB's Cftool. The results can be seen in Table 5.

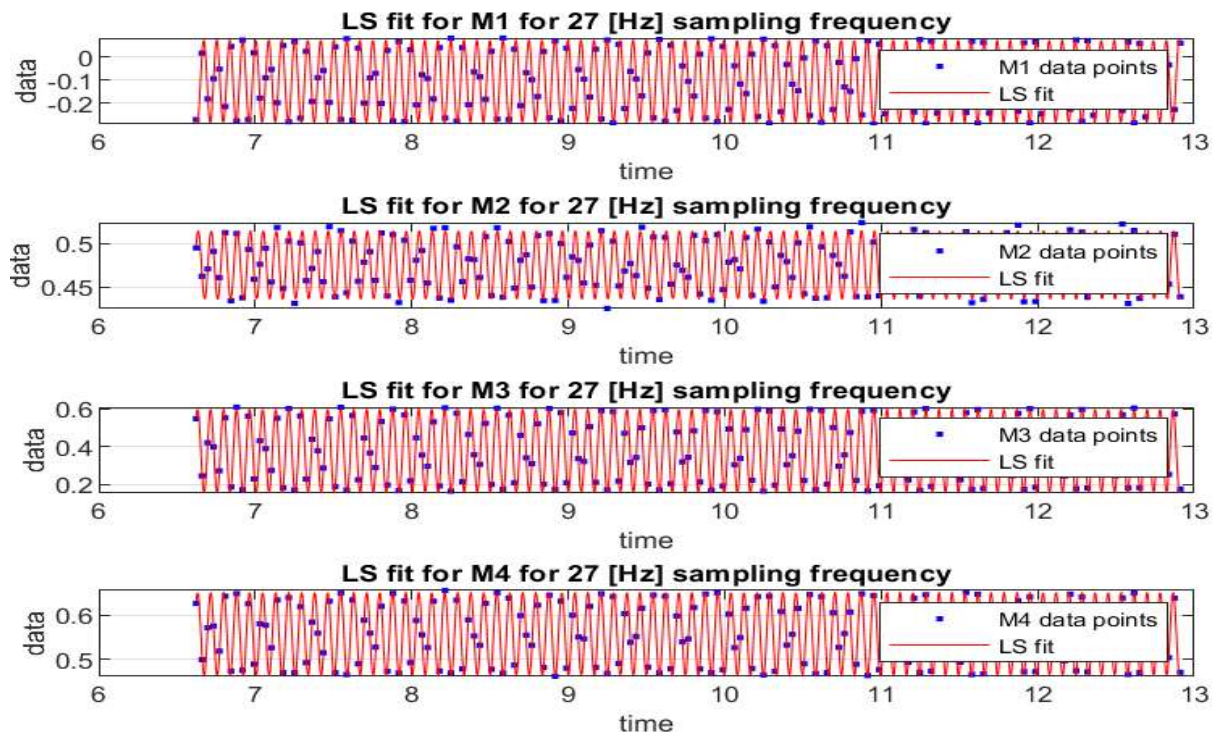


Figure 9: LS fit for $f_s = 27$ [Hz]

Mass	M	f [Hz]	ϕ [rad]	D	R^2
1	0.18	12.03	0.02222	-0.1053	0.9976
2	-0.03967	12.03	-0.4343	0.4752	0.9539
3	-0.2243	12.03	-0.1493	0.3769	0.9949
4	-0.09557	12.03	-0.1675	0.5575	0.9888

Table 5: LS fit results for $f_s = 27$ [Hz]

3.3 33 [Hz] sampling experiment

The Fourier transformation for 33 [Hz] can be seen below.

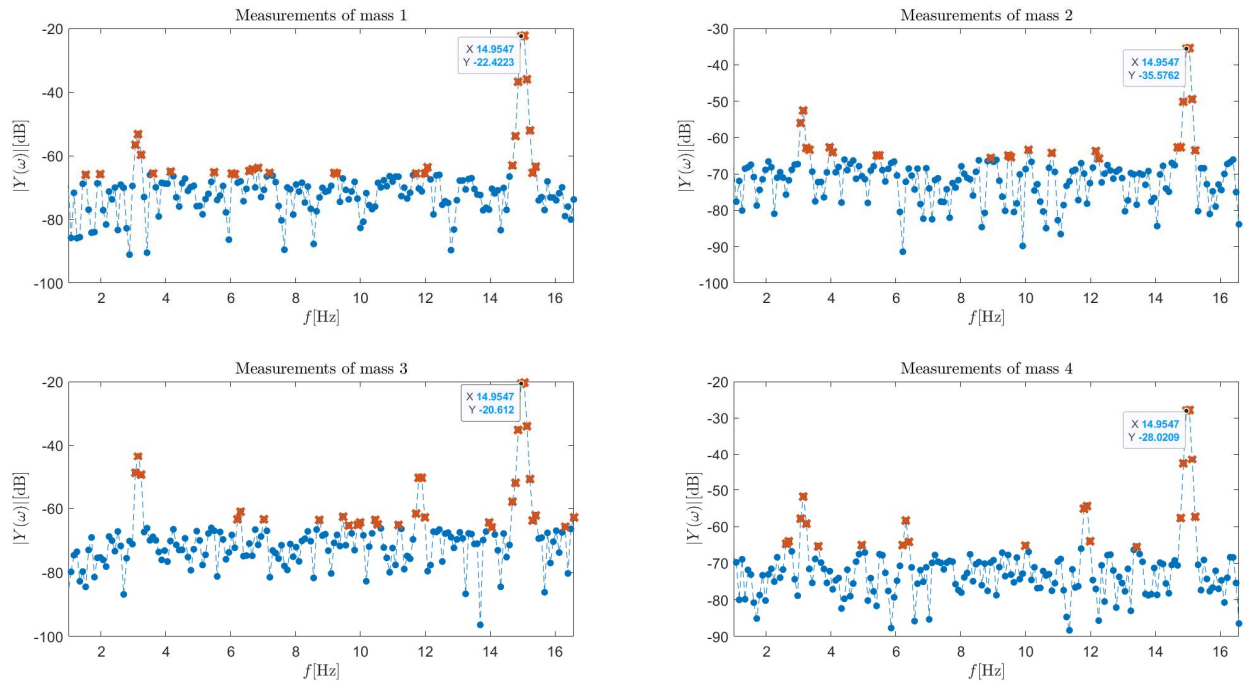


Figure 10: Fourier transformation for $f_s = 33$ [Hz]

We can obtain the amplitude $M = 10^{M_{Db}/20}$. The frequency f [Hz] of the response $y_n = 2M * \sin(2\pi ft)$ is shown in Figure 10.

Mass	2^*M [V]	M [V]	f [Hz]
1	$10^{-\frac{22.4223}{20}} = 0.07566$	0.03783	14.9547
2	$10^{-\frac{35.5762}{20}} = 0.01664$	0.00832	14.9547
3	$10^{-\frac{20.612}{20}} = 0.0932$	0.0466	14.9547
4	$10^{-\frac{28.0209}{20}} = 0.03972$	0.01986	14.9547

Table 6: Fourier transformation results for $f_s = 33$ [Hz]

We will now fit our response to the curve $y_n = M * \sin(2\pi f t + \phi) + D$ using the LS method, where M , ϕ and D are the parameters we'd like to find. This was done using MATLAB's Cftool. The results can be seen in Table 7.

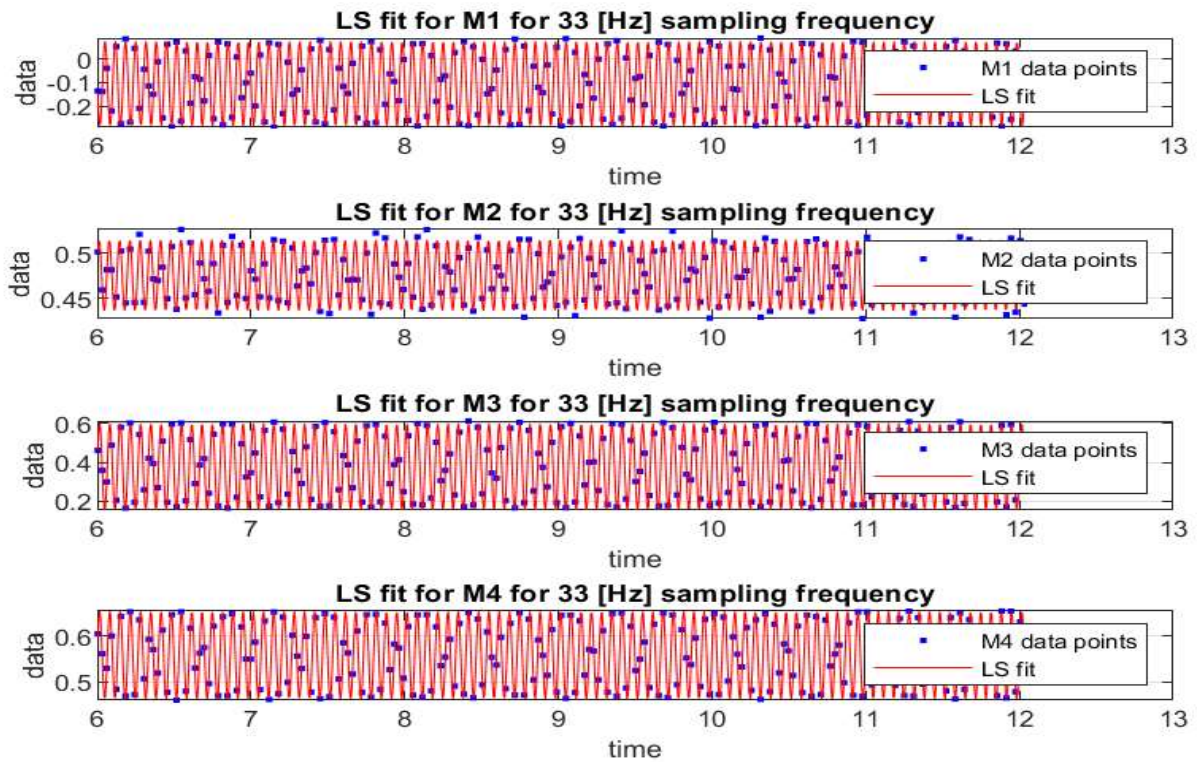


Figure 11: LS fit for $f_s = 33$ [Hz]

Mass	M	f [Hz]	ϕ [rad]	D	R²
1	-0.1803	14.999	0.0162	-0.1048	0.9974
2	0.03915	14.999	0.5047	0.4754	0.9522
3	0.22224	14.999	0.1844	0.3778	0.9935
4	0.09506	14.999	0.2077	0.5581	0.9896

Table 7: LS fit results for $f_s = 33$ [Hz]

3.4 60 [Hz] sampling experiment

The Fourier transformation for 60 [Hz] can be seen below.

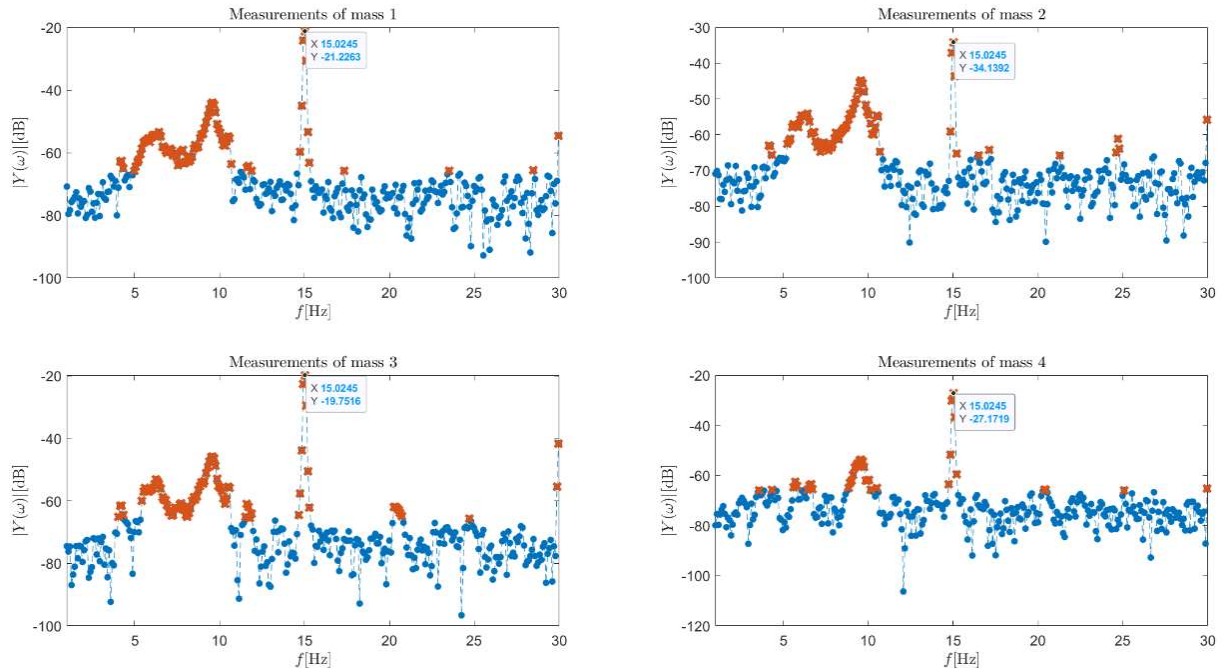


Figure 12: Fourier transformation for $f_s = 60$ [Hz]

We can obtain the amplitude $M = 10^{M_{Db}/20}$. The frequency f [Hz] of the response $y_n = 2M * \sin(2\pi ft)$ is shown in Figure 12.

Mass	2^*M [V]	M [V]	f [Hz]
1	$10^{-\frac{21.2263}{20}} = 0.08683$	0.043416	15.0245
2	$10^{-\frac{-34.1392}{20}} = 0.01964$	0.0098177	15.0245
3	$10^{-\frac{-19.7516}{20}} = 0.1029$	0.05145	15.0245
4	$10^{-\frac{-27.1719}{20}} = 0.04379$	0.02189	15.0245

Table 8: Fourier transformation results for $f_s = 60$ [Hz]

We will now fit our response to the curve $y_n = M * \sin(2\pi f t + \phi) + D$ using the LS method, where M, ϕ and D are the parameters we'd like to find. This was done using MATLAB's Cftool. The results can be seen in Table 9.

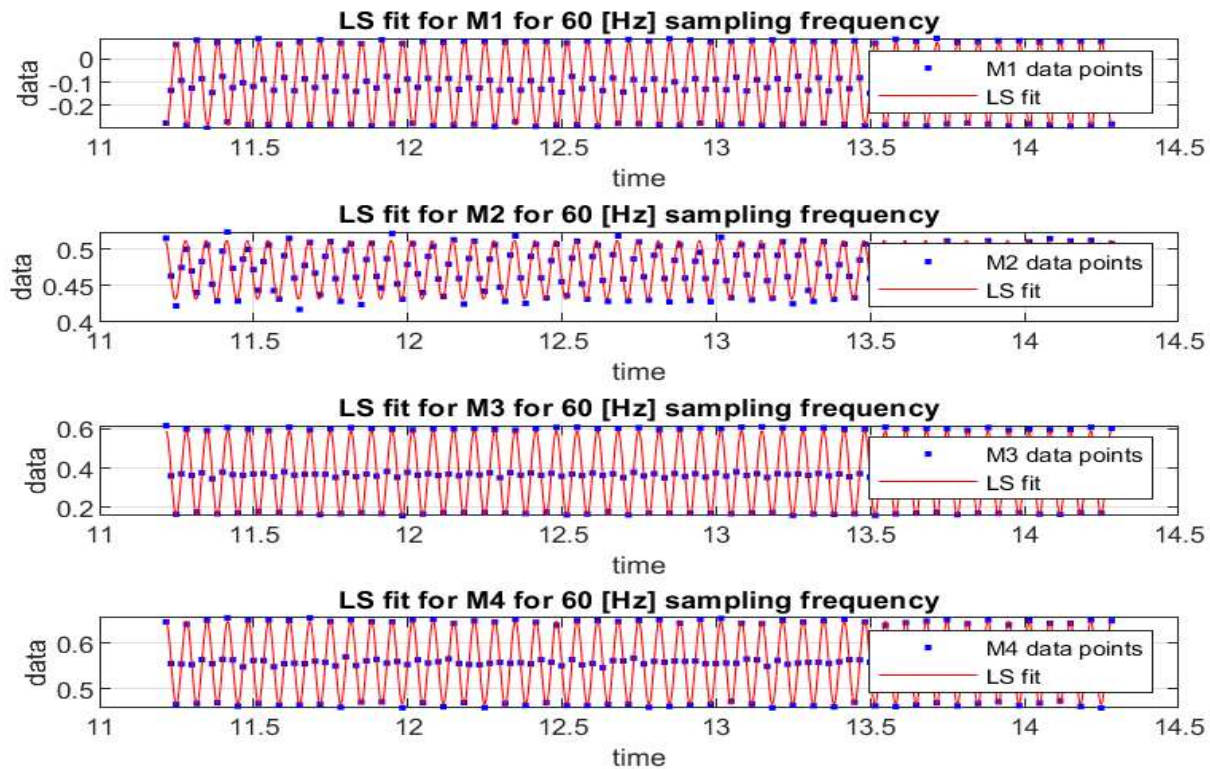


Figure 13: LS fit for $f_s = 60$ [Hz]

Mass	M	f [Hz]	ϕ [rad]	D	R^2
1	-0.1801	15.005	-0.4115	-0.1057	0.9971
2	0.04067	15.005	0.05251	0.4718	0.9598
3	0.2155	15.005	-0.2488	0.3764	0.9947
4	0.09092	15.005	-0.2688	0.5574	0.995

Table 9: LS fit results for $f_s = 60$ [Hz]

3.5 1000 [Hz] sampling experiment

The Fourier transformation for 1000 [Hz] can be seen below.

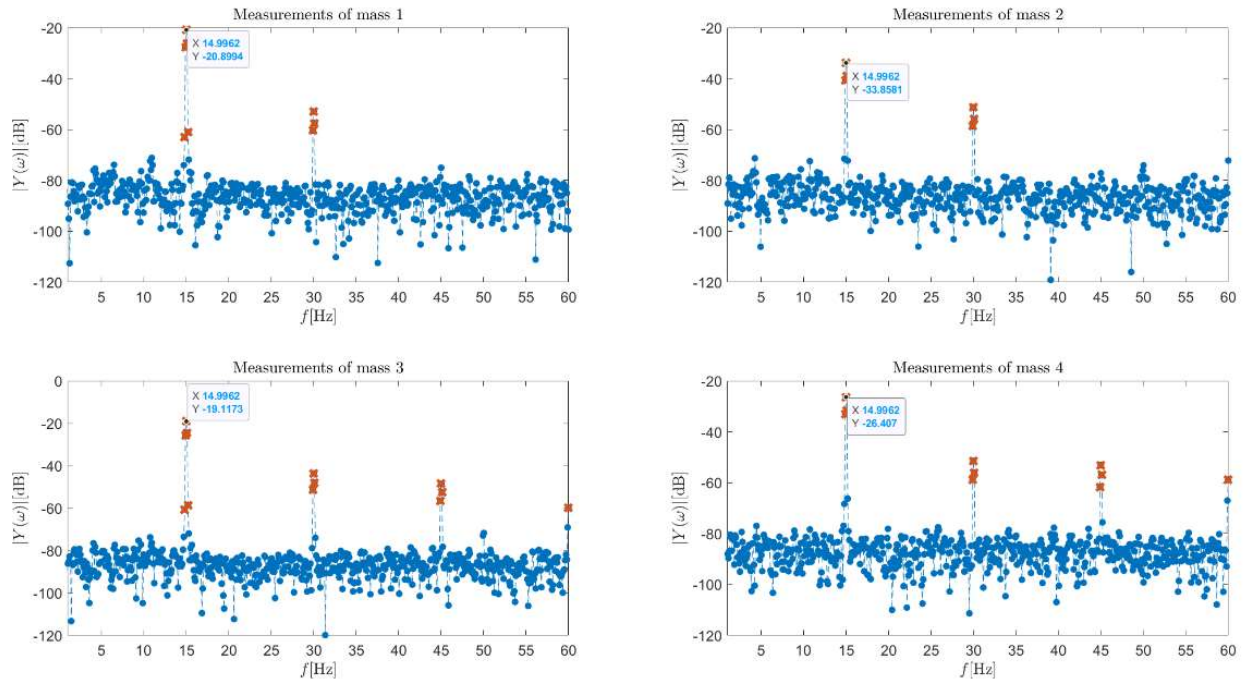


Figure 14: Fourier transformation for $f_s = 1000$ [Hz]

We can obtain the amplitude $M = 10^{M_{Db}/20}$. The frequency f [Hz] of the response $y_n = 2M * \sin(2\pi ft)$ is shown in Figure 14.

Mass	2^*M [V]	M [V]	f [Hz]
1	$10^{-\frac{20.8994}{20}} = 0.09016$	0.04508	14.9962
2	$10^{-\frac{-33.8581}{20}} = 0.020281$	0.01014	14.9962
3	$10^{-\frac{-19.1173}{20}} = 0.110697$	0.055348	14.9962
4	$10^{-\frac{-26.407}{20}} = 0.047824$	0.02391	14.9962

Table 10: Fourier transformation results for $f_s = 1000$ [Hz]

We will now fit our response to the curve $y_n = M * \sin(2\pi f t + \phi) + D$ using the LS method, where M, ϕ and D are the parameters we'd like to find. This was done using MATLAB's Cftool. The results can be seen in Table 11.

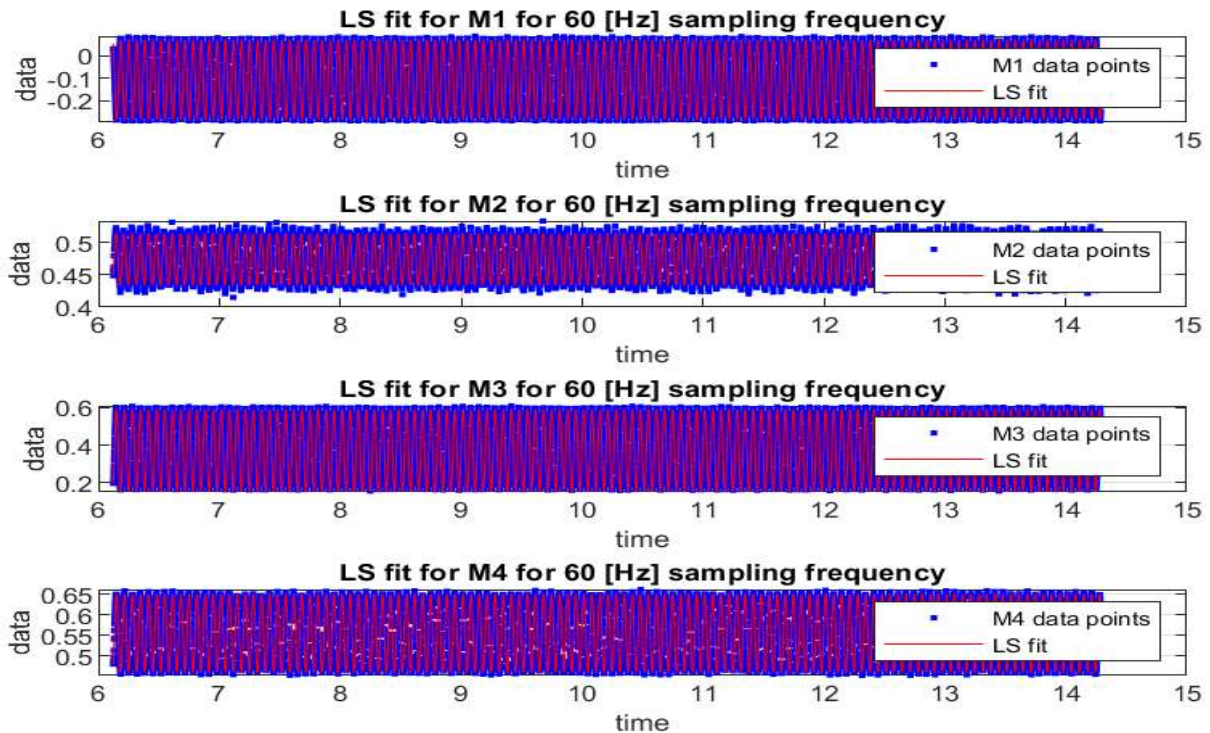


Figure 15: LS fit for $f_s = 1000$ [Hz]

Mass	M	f [Hz]	ϕ [rad]	D	R^2
1	-0.1803	15.005	-0.3564	-0.1058	0.9954
2	0.04062	15.005	0.1194	0.474	0.9545
3	0.2215	15.005	-0.1827	0.3714	0.9916
4	0.09569	15.005	-0.1634	0.5555	0.9869

Table 11: LS fit results for $f_s = 1000$ [Hz]

3.6 Sampling experiment Summary

The following table summarizes the results from the sampling experiments, taking the average magnitude and frequency of the 4 masses, for both the Fourier model and the LS model.

f_s [Hz]	$\bar{M}_{Fourier}$ [V]	\bar{M}_{LS} [V]	$\bar{f}_{Fourier}$ [Hz]	\bar{f}_{LS} [Hz]
11	0.031779	0.04479	4.02117	3.989
27	0.03066	0.044885	11.9927	12.03
33	0.02815	0.0440775	14.9547	14.999
60	0.031643	0.0417475	15.0245	15.005
100	0.0336195	0.0443775	14.9962	15.005

We can see, that for the frequencies 11 [Hz] and 27 [Hz], they do not satisfy the Nyquist criterion, & therefore the reconstructed frequencies do not match the 15 [Hz] input frequency. This is due to aliasing, which causes the sampled signal to appear at a different frequency. The 3 other sampling frequencies adhere to the criterion and have very close to 15 [Hz] frequencies.

The magnitudes of the LS method for different sampling frequencies are all very close to each other. The magnitudes of the Fourier model for different sampling frequencies are also very close to one another. But the LS method magnitudes & the Fourier model magnitudes are not close to each other. This can be attributed to the inherent characteristics of the Fourier & the LS method in processing and representing data.

4. Linearity verification

A system is linear if following properties of the linear operator are true:

$$L[a_1 u_1(t) + a_2 u_2(t)] = a_1 * L[u_1(t)] + a_2 * L[u_2(t)] = a_1 y_1(t) + a_2 y_2(t)$$

To check if our system is linear, we input two sinusoidal signals with different frequencies, summed their response, and compared that to the system response for an input signal equal to the linear composition of the two sinusoidal signals. The two sine input signals are:

$$u_1 = a_1 \sin(2\pi f_1 t)$$

$$u_2 = a_2 \sin(2\pi f_2 t)$$

$$f_1 = 2 \text{ [Hz]}, f_2 = 6 \text{ [Hz]}, a_1 = 0.3, a_2 = 0.5$$

The results can be seen below.

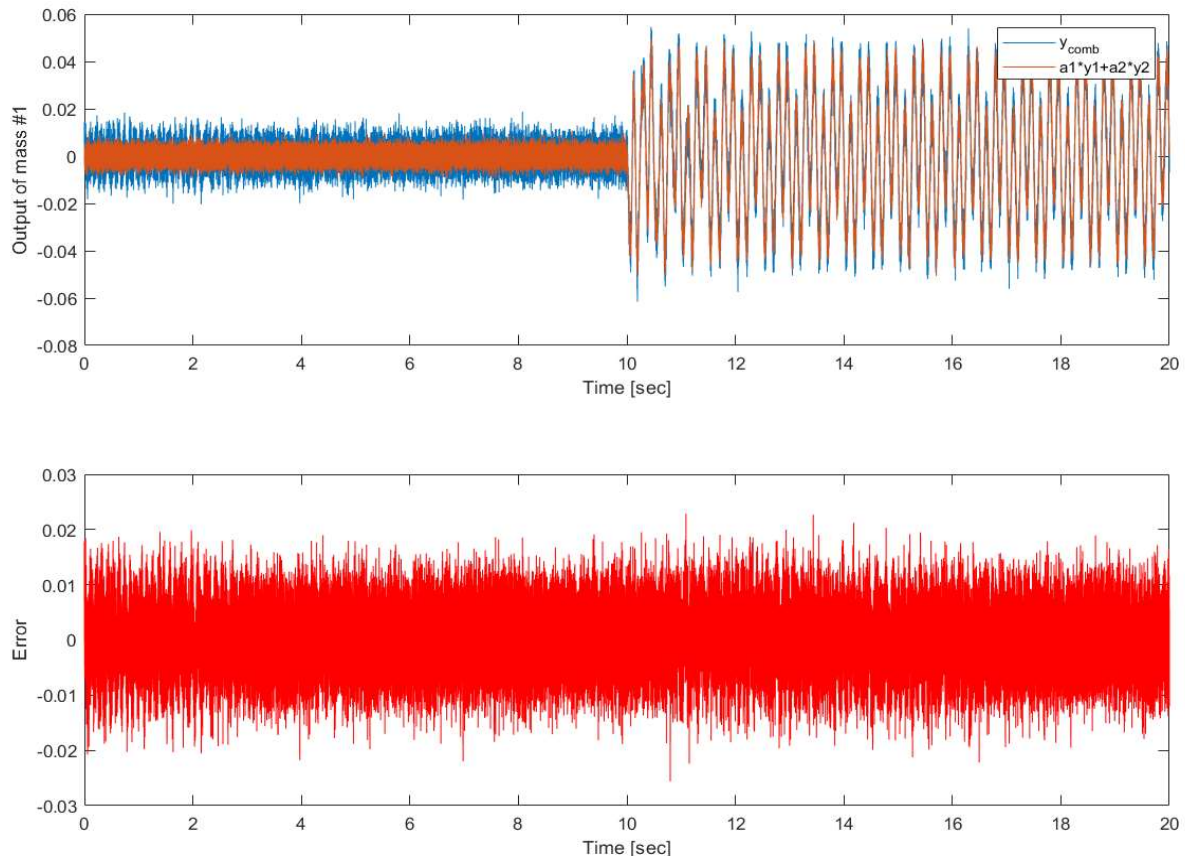


Figure 16: Linearity verification for low amplitudes

The top graph shows the systems response with the $y_{comb} = 0.3 \sin(2\pi * 2t) + 0.5 \sin(2\pi * 6t)$, and the sum of two individual sinusoidal inputs $0.3 \sin(2\pi * 2t)$ and $0.5 \sin(2\pi * 6t)$. The bottom graph shows the error between these 2 responses. We can see that the error is relatively small, and that the magnitude stays the same before and after the 10 [sec] mark, which is when the system starts operating. This means the error is due to measurement noise only. The system is therefore linear.

We tried the same experiment, but with much higher amplitudes of $a_1 = 3$ and $a_2 = 5$, while keeping the same frequencies. The results can be seen below.

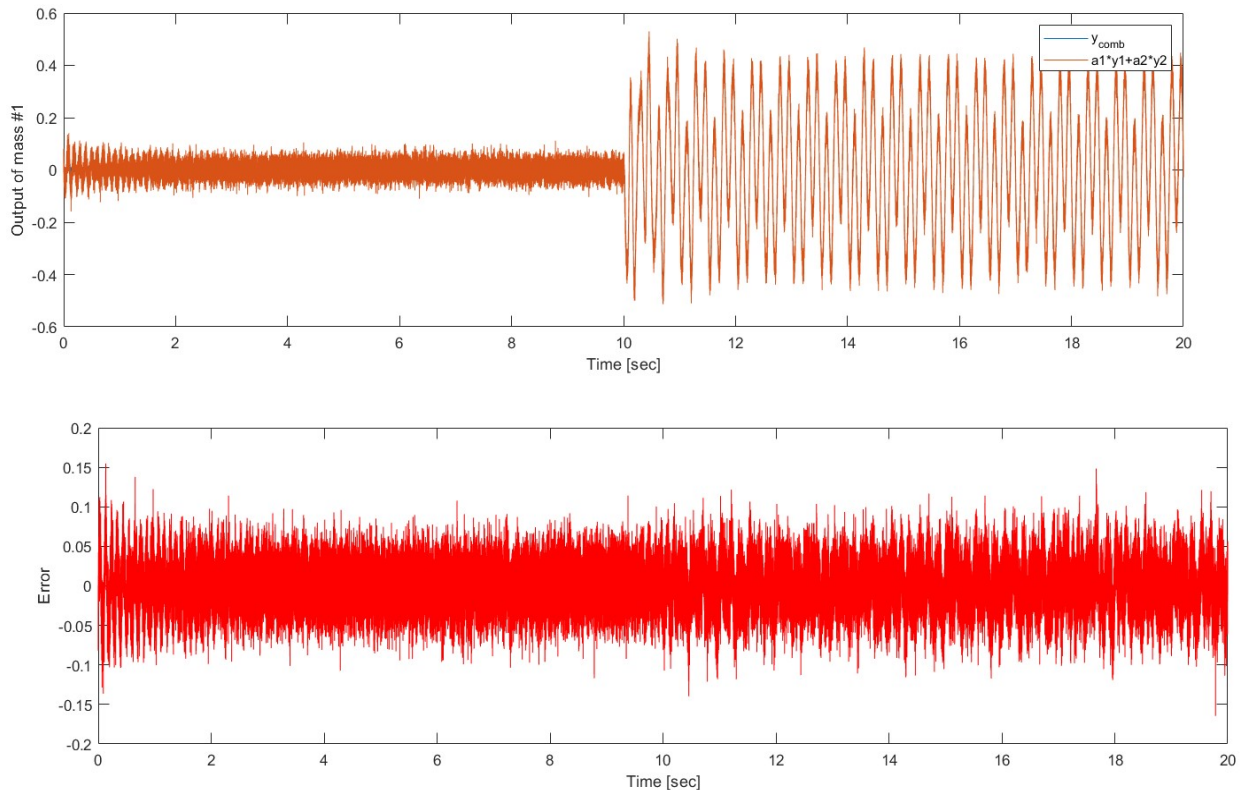


Figure 17: Linearity verification for high amplitudes

We can derive the same conclusions from both these graphs. The error of these amplitudes has a similar ratio to the outputs, then with the smaller amplitudes. We can also see that the error is the same before and after the 10 [sec] mark, which means the error is measurement noise, and the system is linear.

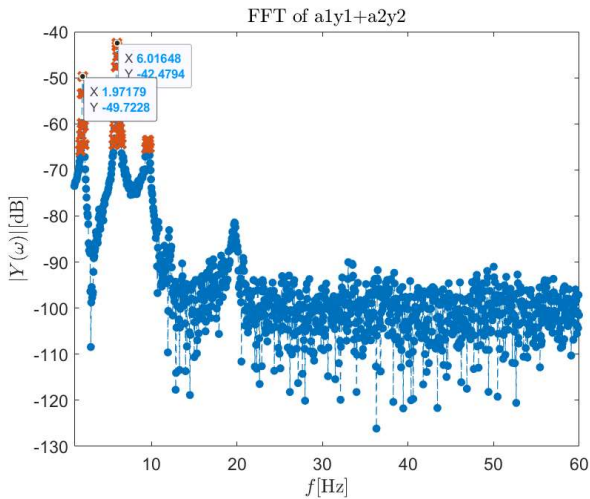


Figure 19: FFT of $a_1y_1 + a_2y_2$

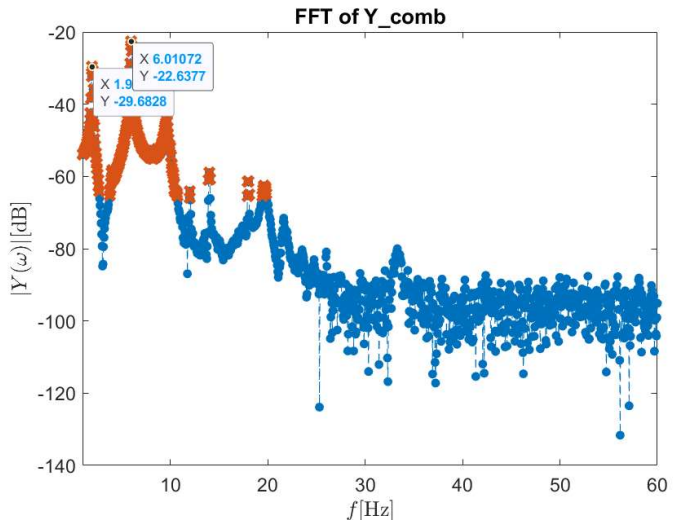


Figure 18: FFT of y_{comb}

From both FFT transformations with the low amplitudes $a_1 = 0.3$ and $a_2 = 0.5$, we can see that both have similar dominant frequencies.

5. Natural Frequencies using Step response

To find the natural frequencies of the system, we applied a step response to the system, and analyzed the response using a Fourier transform. This allowed us to find the dominant frequencies in the system. The dominant frequencies for each mass can be found below.

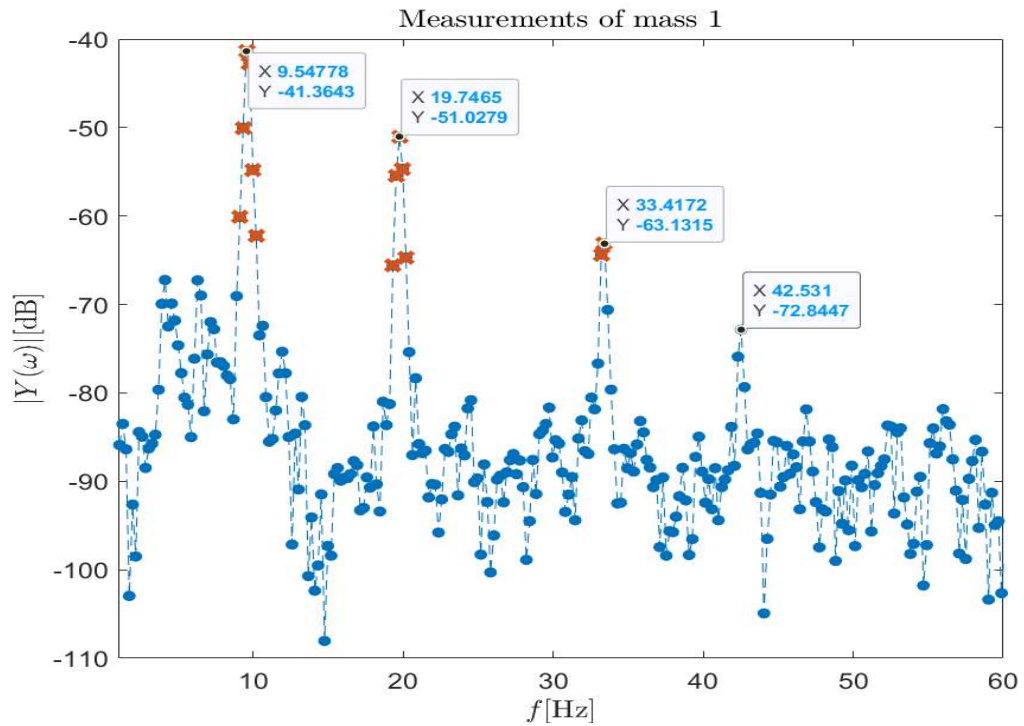


Figure 20: Natural frequencies of mass 1

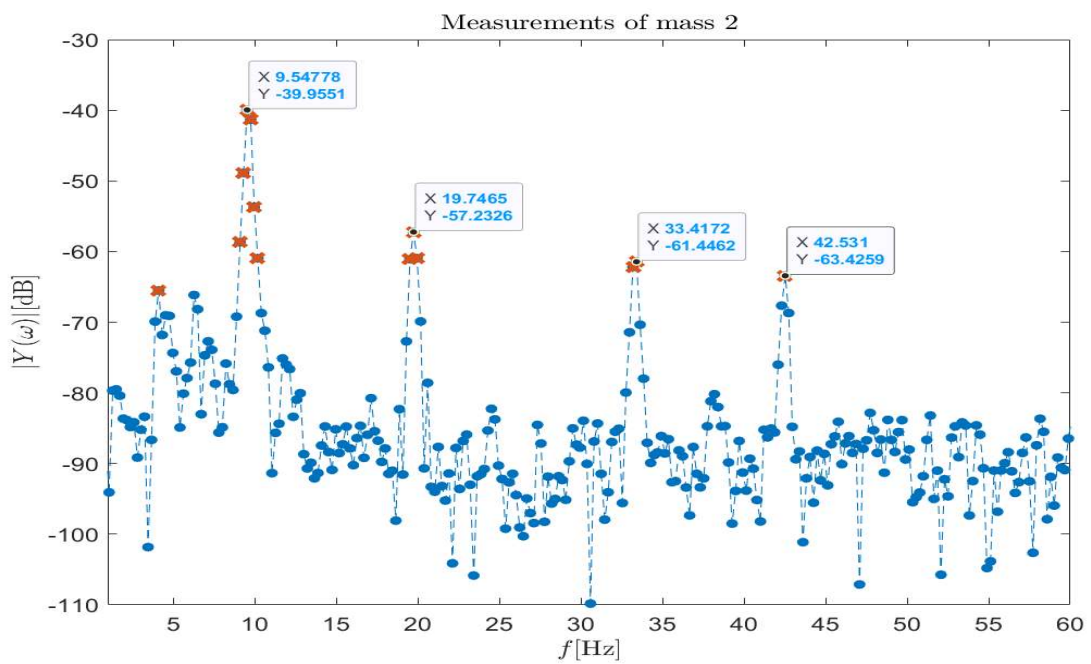


Figure 21: Natural frequencies of mass 2

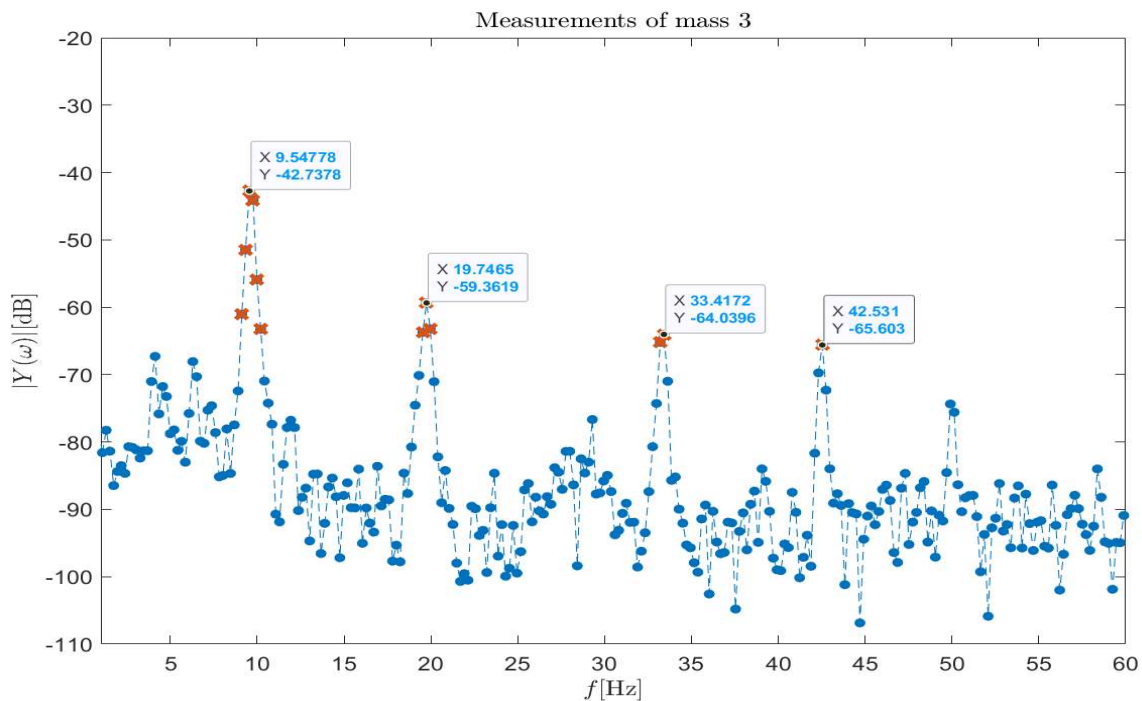


Figure 22: Natural frequencies of mass 3

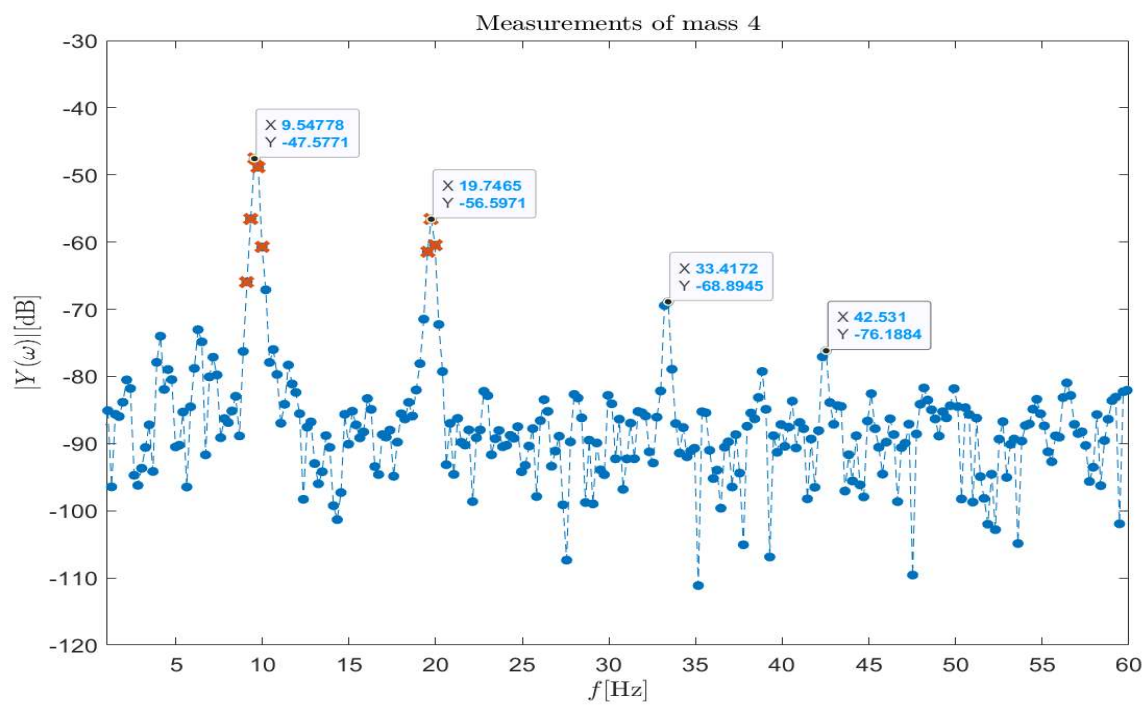


Figure 23: Natural frequencies of mass 4

Mass	f_{n1}	f_{n2}	f_{n3}	f_{n4}
Theoretical value:	10.1559	19.587	32.57	41.689
1	9.54778	19.7465	33.4172	42.531
2	9.54778	19.7465	33.4172	42.531
3	9.54778	19.7465	33.4172	42.531
4	9.54778	19.7465	33.4172	42.531
Relative Error (%)	5.99 %	0.81 %	2.6 %	2.02 %

Table 12: Natural frequencies for all masses

The relative error has been calculated using following formula:

$$\text{Error [%]} = \left| \frac{f_{theoretica} - f_{experimental}}{f_{theoretica}} \right| * 100\%$$

The relative error obtained in our experiment are small, and may be due to many factors, like measurement noise.

6. Eigenvector analysis

To investigate the eigenvectors, we will measure the displacement of all masses simultaneously, and compare the amplitudes and phases of the displacements of every mass relative to the other masses. We will apply a sinusoidal signal excitation for each of the natural frequencies found in previous section. We will start with the first natural frequency of $f_{n1} = 10$ [Hz]. The outputs of all four masses, together with the voltage in the actuator, have been plotted individually and can be seen in the Figures below. The LS results can be seen in Table 13.

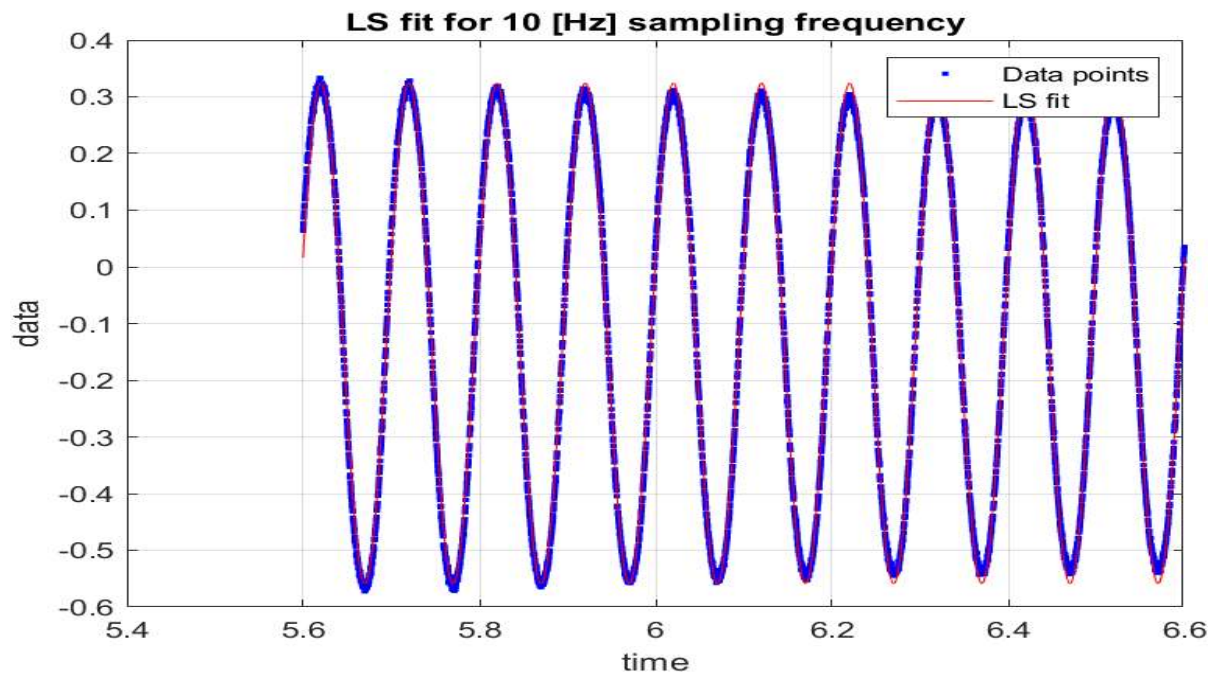


Figure 24: Displacement of Mass 1 with an input signal of $f_{n1} = 10$ [Hz]

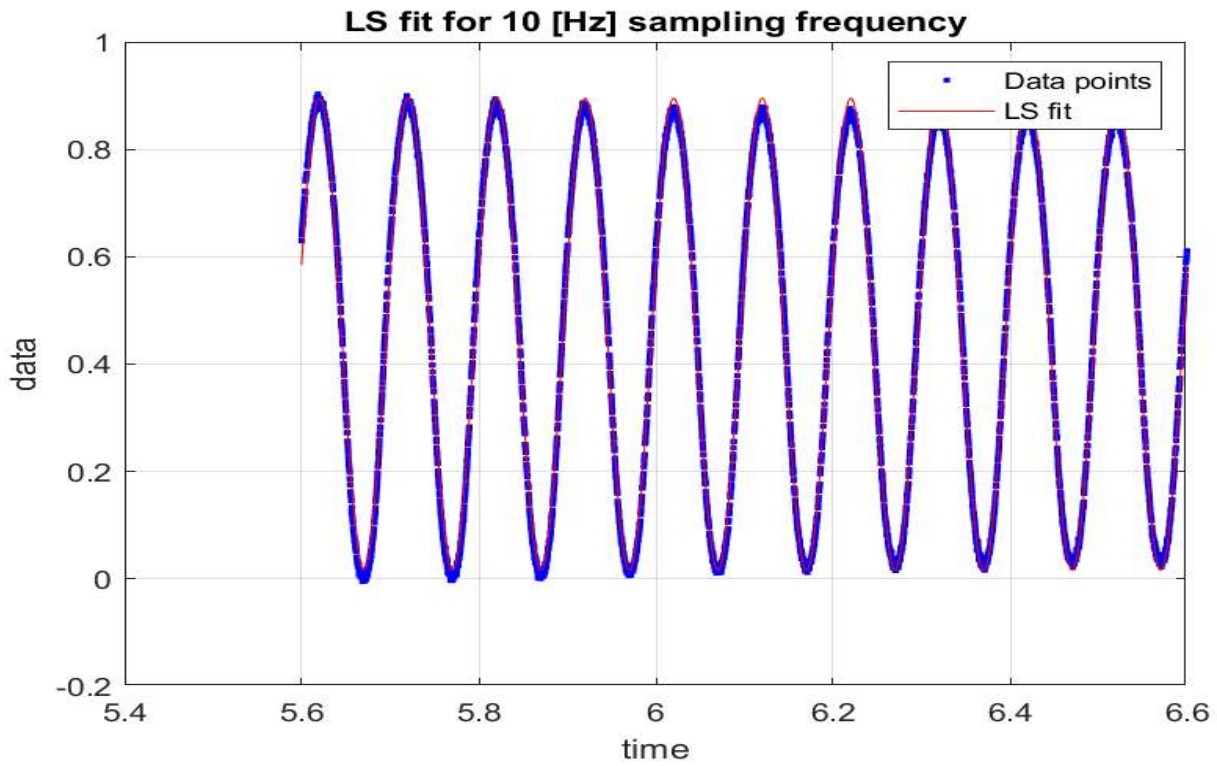


Figure 25: Displacement of Mass 2 with an input signal of $f_{n1} = 10$ [Hz]

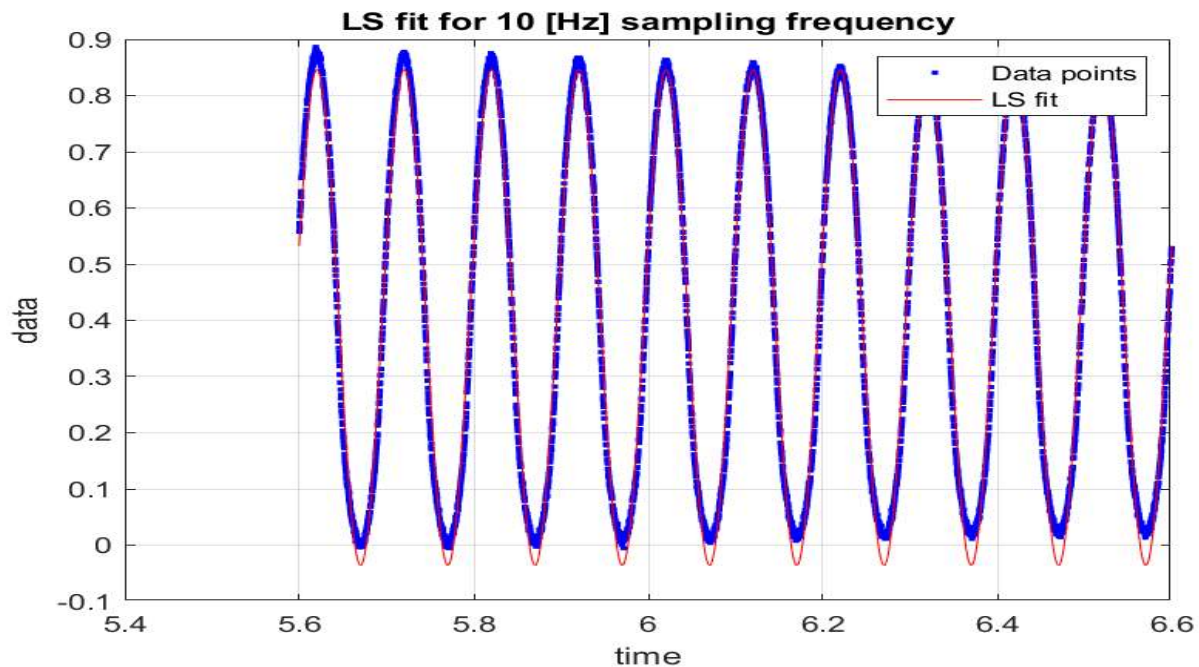


Figure 26: Displacement of Mass 3 with an input signal of $f_{n1} = 10$ [Hz]

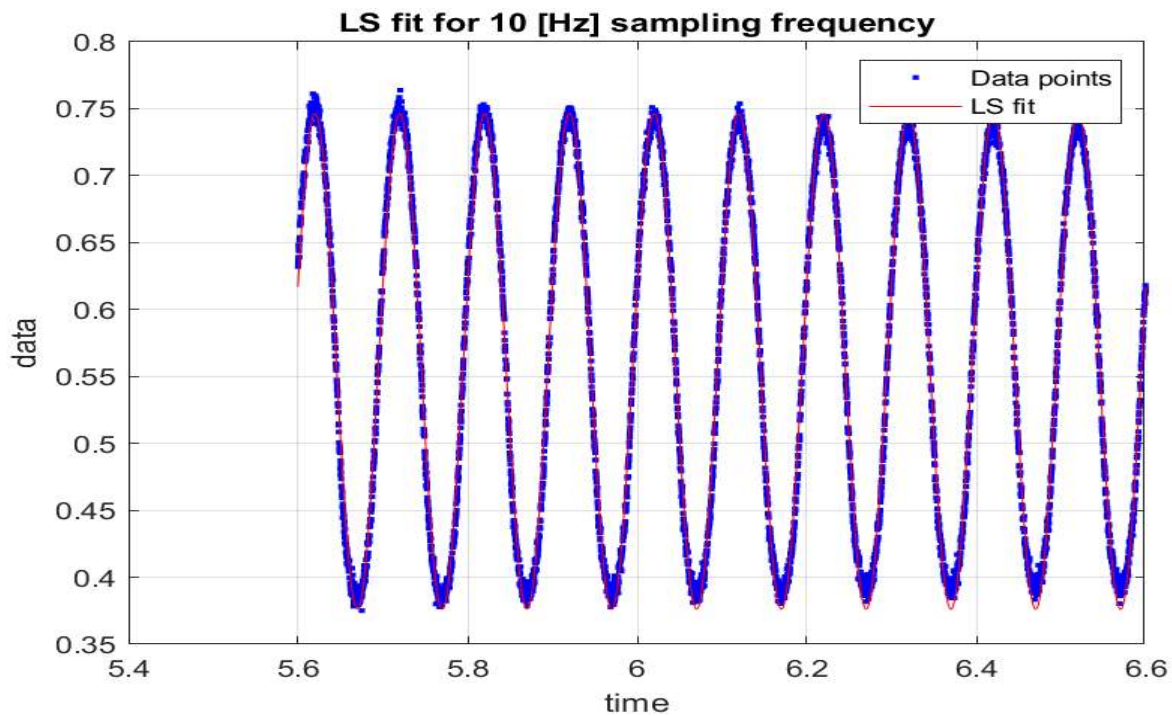


Figure 27: Displacement of Mass 4 with an input signal of $f_{n1} = 10$ [Hz]

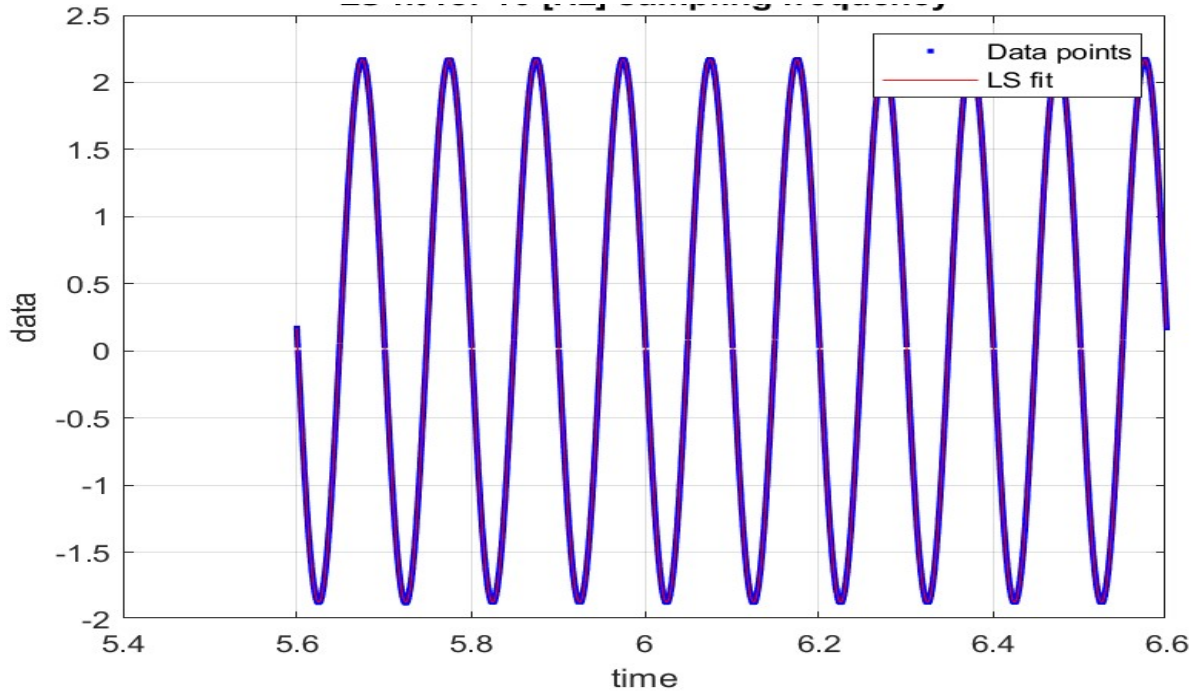


Figure 28: Voltage of the actuator, $V_c = 2$ [V]

Mass	M	f_{n1} [Hz]	ϕ [rad]	D	R^2
1	0.4415	10	0.3189	-0.1173	0.997
2	0.4398	10	0.3091	0.4558	0.9964
3	0.441	10	0.3055	0.4052	0.9898
4	0.1852	10	0.3177	0.5613	0.9952
Actuator	-2.021	10	0	0.1485	1

We can see that the phases of all 4 masses are very close to each other.

The following eigenvectors were obtained analytically:

$$\vec{v}_1 = \begin{bmatrix} -0.9129 \\ -0.9129 \\ -0.9129 \\ -0.9129 \end{bmatrix}; \vec{v}_2 = \begin{bmatrix} 1.1927 \\ 0.4940 \\ -0.4940 \\ -1.1927 \end{bmatrix}; \vec{v}_3 = \begin{bmatrix} 0.9129 \\ -0.9129 \\ -0.9129 \\ 0.9129 \end{bmatrix}; \vec{v}_4 = \begin{bmatrix} -0.4940 \\ 1.1927 \\ -1.1927 \\ 0.4940 \end{bmatrix}$$

We excited the setup with sinusoidal excitation at each of the natural frequencies and measured the voltage across all 4 masses.

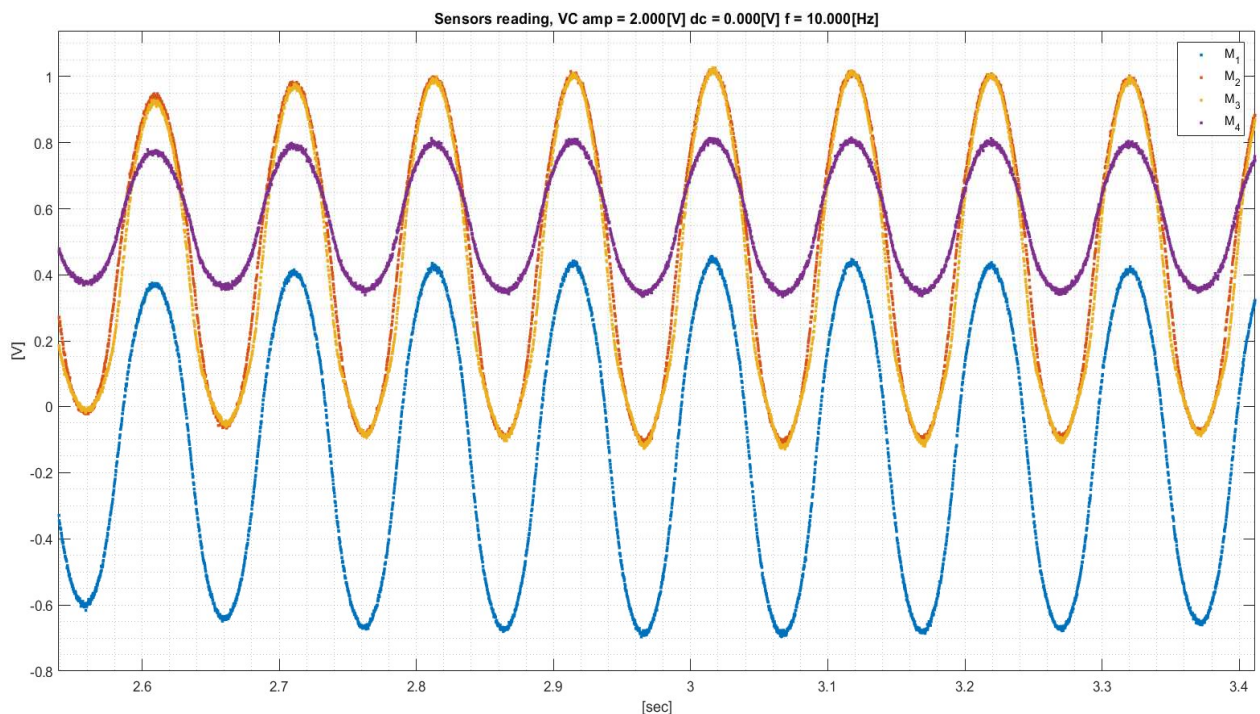


Figure 29: Sine response for $f_n = 10$ [Hz]

In Figure 29, we can see that all 4 masses move in the same phase. This is in accordance with eigenvector \vec{v}_1 , where all values in the vector are negative.

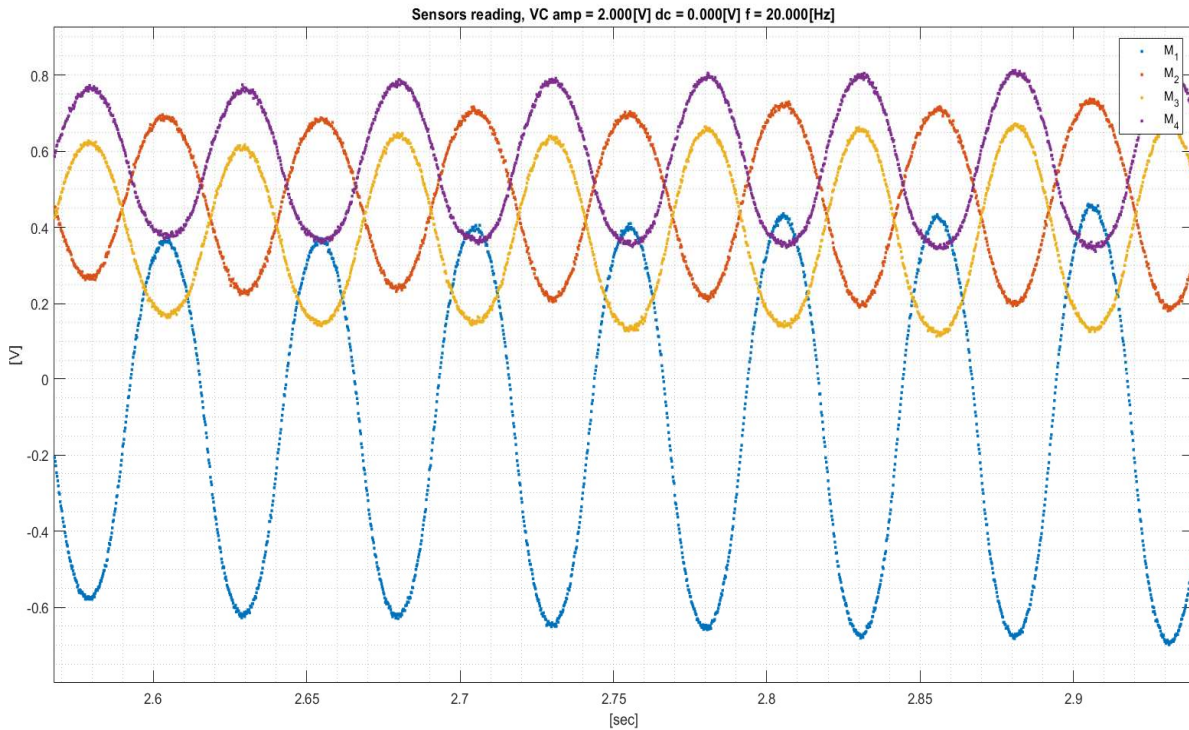


Figure 30: Sine response for $f_n = 20$ [Hz]

In Figure 30, we can see that Masses 1 & 2 move in the same phase, while Masses 3 & 4 move in an anti-phase. This is in accordance with eigenvector \vec{v}_2 , where the first two values are positive, while the last two values are negative.

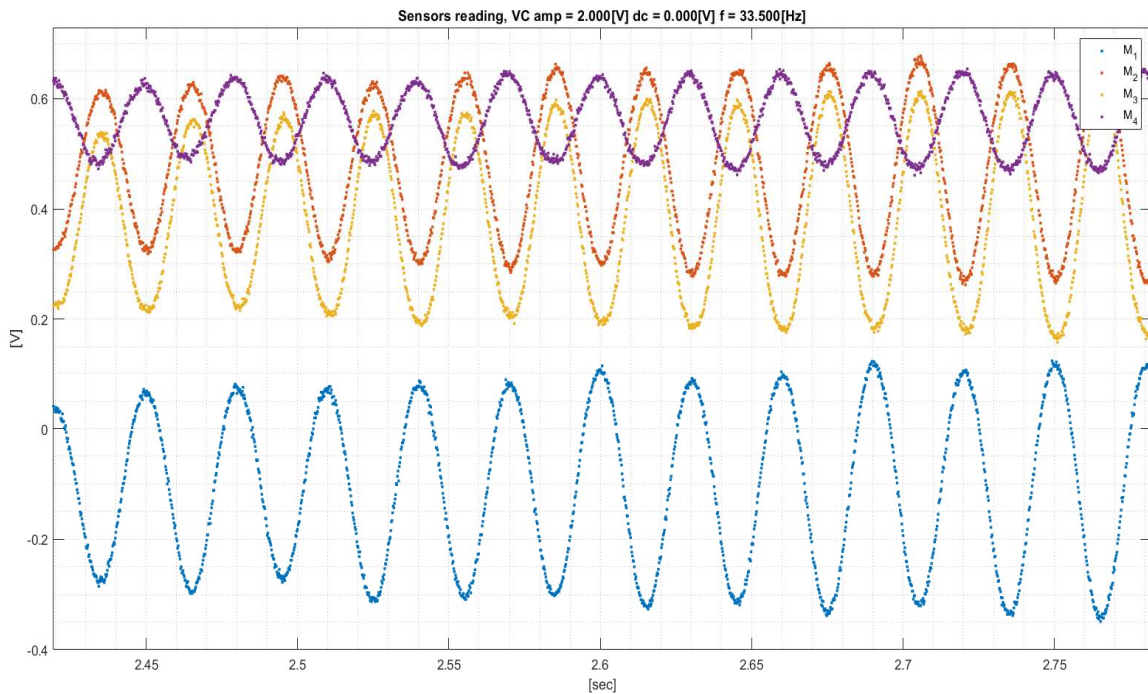


Figure 31: Sine response for $f_n = 33.5$ [Hz]

In Figure 31, we see masses 1 & 4 move in the same phase, and masses 2 & 3 move in anti-phase. This is in accordance with eigenvector \vec{v}_3 , where the first & last value are positive, while the middle two values are negative.

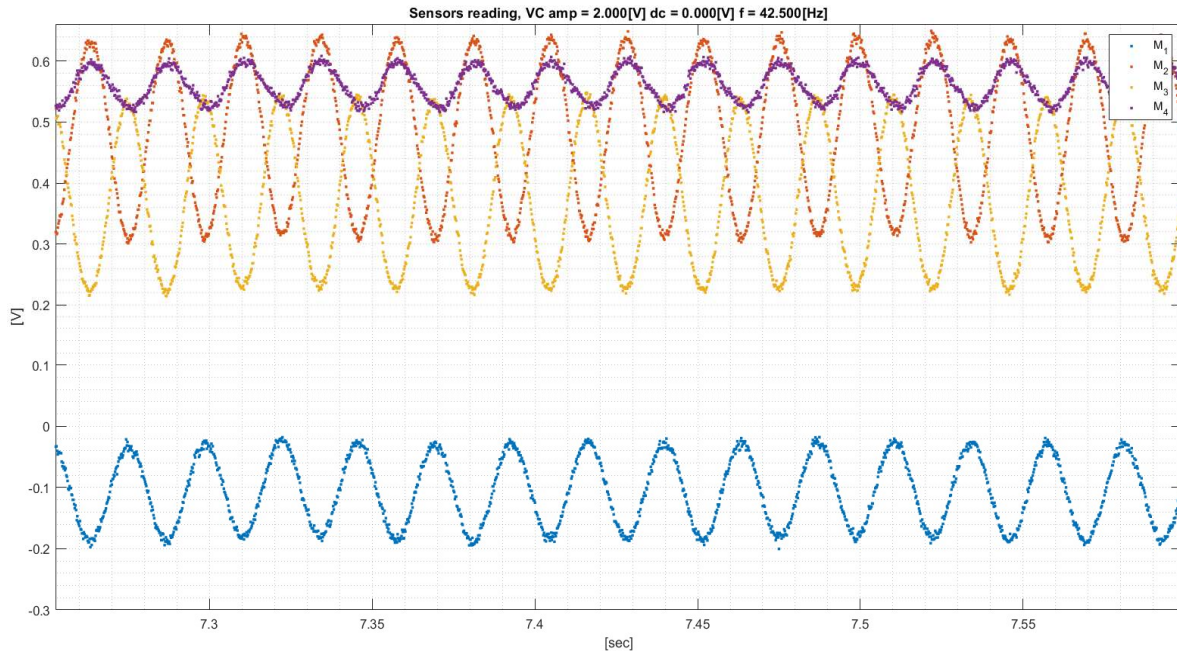


Figure 32: Sine response for $f_n = 42$ [Hz]

In Figure 32, we see masses 1 & 3 move in the same phase, and masses 2 & 4 in anti-phase. This is in accordance with eigenvector \vec{v}_4 , where the first & third values are negative, while the second & fourth values are positive.

7. Summary

In this lab, we focused on characterizing vibrating systems by determining their natural frequencies, eigenvectors, and damping coefficients. The key experiments conducted and their main conclusions are outlined below:

Sensor Calibration

The calibration of the sensors was performed to ensure accurate and reliable measurements. Calibration curves showed a linear relationship with high accuracy for all four masses.

Sampling Experiment

The system was excited with a sine wave at 15 Hz, and the response was sampled at various frequencies. The results highlighted the importance of the Nyquist criterion to avoid aliasing. Frequencies below 30 Hz did not satisfy the criterion and resulted in aliasing, while higher frequencies provided accurate representations of the signal.

Linearity Verification

The linearity of the system was verified by comparing the response to a linear combination of two sinusoidal inputs with the sum of their individual responses. The results confirmed the system's linearity within the tested range, as the error was attributed to measurement noise only.

Natural Frequencies Using Step Response

A step response was applied to the system, and the resulting Fourier transform was used to identify the dominant frequencies. The experimental values closely matched the theoretical natural frequencies, with small relative errors likely due to measurement noise.

Eigenvector Analysis

Sinusoidal excitation at the natural frequencies allowed us to analyze the phase and amplitude relationships between the masses. The experimental results were consistent with the analytical eigenvectors, confirming the modal behavior of the system.

Advanced Laboratory in Mechanical Engineering (034057)

Lab 2: Vibrations

05/06/2023

Lab Instructor: Aharon Levin



Due date: 24.06.2024

E-mail	ID	Name
dannyapsel@campus.technion.ac.il	931203285	Danny Apsel
Sagi.chen@campus.technion.ac.il	209408673	Sagi Chen

We did not receive any consultation/discussion with members of other groups or with students who took the course in the past. We did not use a report/project that was written in previous semesters (reference). We did not use a tool based on artificial intelligence such as Chat GPT.

Table of Contents

1.	Introduction	3
1.1	Experimental setup.....	3
1.2	Lab objectives	4
2.	Frequency response experiment	6
2.1	Bode Diagrams.....	6
2.2	Nyquist plots analysis	10
3.	Damping effect investigation using Q-factor.....	13
4.	Decay envelope measurement	17
4.1	Low damping	17
4.2	High damping.....	20
5.	Summary.....	23
5.1	Frequency response	23
5.2	Damping effect investigation using Q-factor.....	23
5.3	Decay Envelope Measurement.....	23

1. Introduction

1.1 Experimental setup

Figure 1 shows an image of the experimental setup, which consists of flexible elements, including straight and arched spring elements, connecting rigid metal blocks (masses) to form a structure where there is a mutual influence between the different masses, springs, and the excitation system. Moving one mass causes the other masses to move due to forces exerted by the flexible elements. Dynamic forces in the x-direction can be applied via an electromagnetic actuator (voice coil).

The experimental system includes several additional components. Laser-based optical sensors, where the laser beam is tilted by the movement of each mass, and electronic sensors produce a voltage correlated to the relative position of one of the masses in the x-direction. There is a micrometric system that allows control of the magnet distance from the mass surface, creating forces opposite to the relative velocity between masses and the magnet, which act as damping forces on each mass separately. An electronic card controlled by a computer, using MATLAB during the experiment, converts the four sensor voltages into vectors that can be translated into equivalent engineering sizes (displacement in [mm]) through a process called sampling. Additionally, an electrical signal can be generated for actuating the voice coil, and the current passing through the electromagnet coil can be measured. The actuator force is proportional to the current and can be calibrated.



Figure 1: Experimental setup

1.2 Lab objectives

The primary objective of this lab was to investigate the dynamic response of an oscillatory system by performing three distinct experiments. Each experiment was designed to provide an understanding of the system's behavior under various conditions, focusing on natural frequencies, damping effects, and damping ratio calculations.

Experiment 1: Bode Plot Measurement Using Stepped Sine Testing

This experiment aimed to characterize the system's frequency response by generating Bode plots. Bode plots are instrumental in depicting the amplitude and phase response of the system as a function of frequency. The experiment was conducted in two phases: a coarse scan over a broad frequency range with 0.5 [Hz] increments, followed by fine scans of 0.07 [Hz] increments around the identified natural frequencies. The goal was to find the system's natural frequency and estimate measurement errors by comparing the experimental results with the analytical values, calculated in the pre-lab assignment.

Experiment 2: Investigation of Damping Effect Using Q-factor

The second experiment focused on examining the damping effect within the system by calculating the Q-factor, a crucial parameter in describing the degree of damping. It was determined by analysing the width of the peaks in the Bode plots around the natural frequencies. This experiment involved two setups: the low damping, where the magnets are extremely far from the masses, and increased damping, where the magnets are at a distance of 0.1 [mm] from the masses. The results gave us insights into the relationship between damping ratios and natural frequencies, as well as the impact of damping on system behavior.

Experiment 3: Damping Ratio Calculation Using Decay Envelope

In this experiment, the damping ratio was calculated through decay envelope measurements. By applying a sinusoidal excitation at the system's first natural frequency until a steady state was reached, and then abruptly stopping the excitation, the decay of the system's response was recorded. This process was repeated for both damping conditions from Experiment 2. The decay envelope was fitted with an exponential function to determine the decay constant (τ), from which the damping ratio was derived. Then, the damping ratios between the decay measurements and Q-factor are compared.

2. Frequency response experiment

2.1 Bode Diagrams

In this experiment, we measured the systems frequency response to a sinusoidal input in a frequency range of 5 – 45 [Hz]. The scan was made with intervals of 0.5 [Hz], from frequency to frequency. The results can be seen in Figure 2.

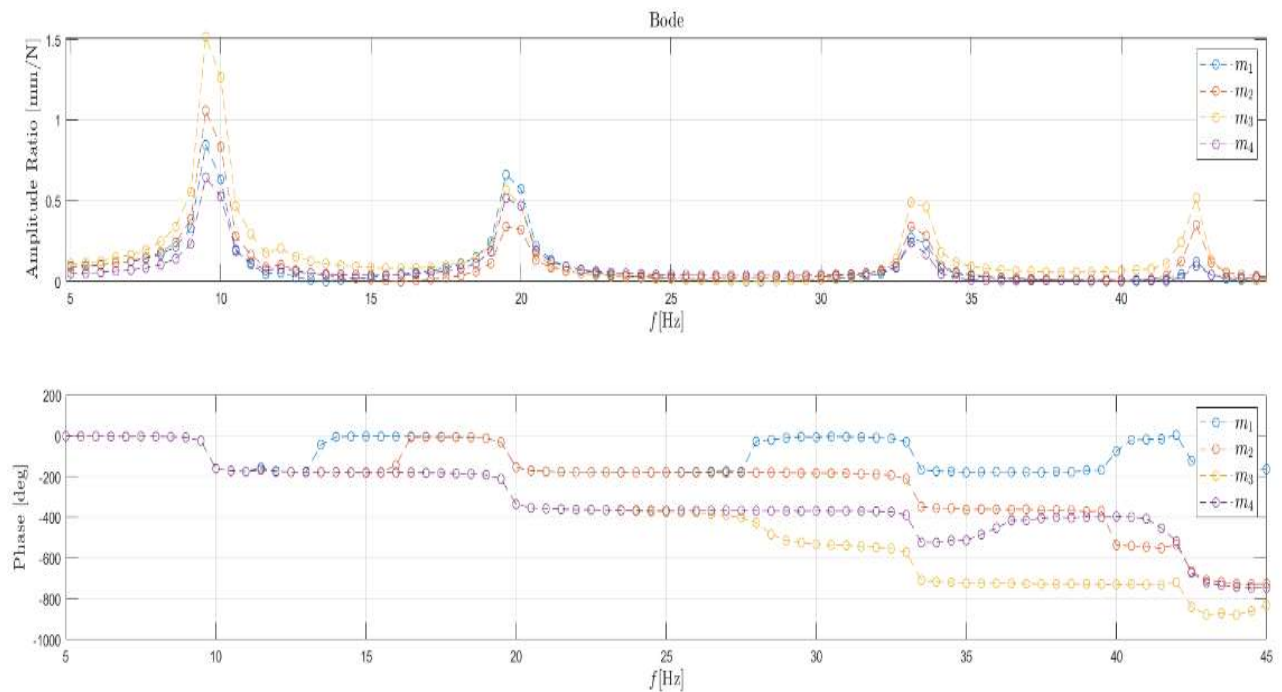


Figure 2: Bode diagram of frequency response of all masses, with steps of 0.5 [Hz]

We can see that our resonant frequencies are around (9.5 [Hz]; 19.5 [Hz]; 33 [Hz]; 42 [Hz]). To get a better view, we will redo the experiment around these resonant frequencies, with a finer step interval of 0.07 [Hz]. The results can be seen below.

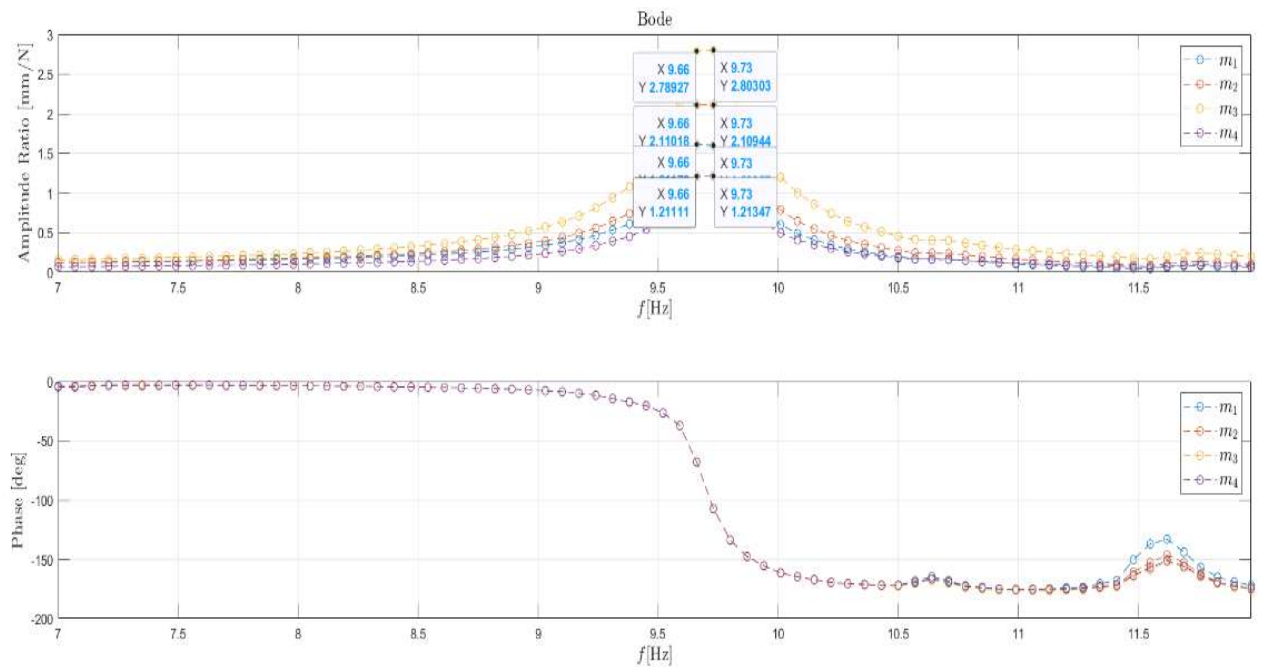


Figure 3: Bode diagram of frequency response of all masses around 9.5 [Hz], with steps of 0.07 [Hz]

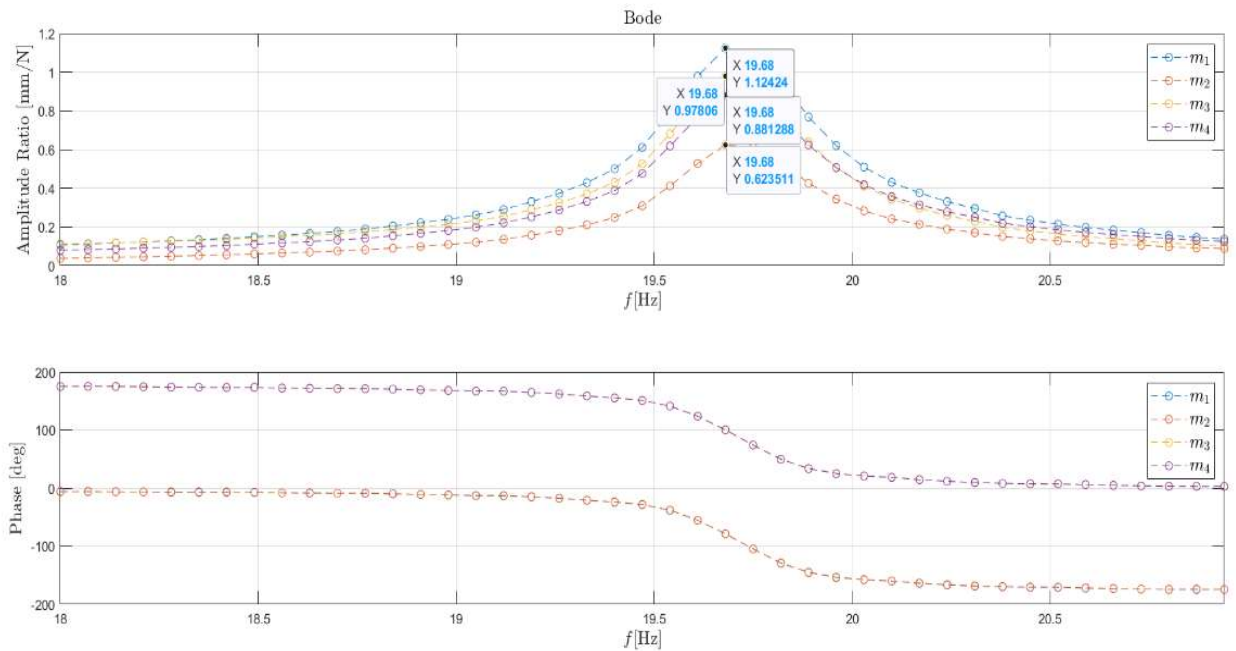


Figure 4: Bode diagram of frequency response of all masses around 19.5 [Hz], with steps of 0.07 [Hz]

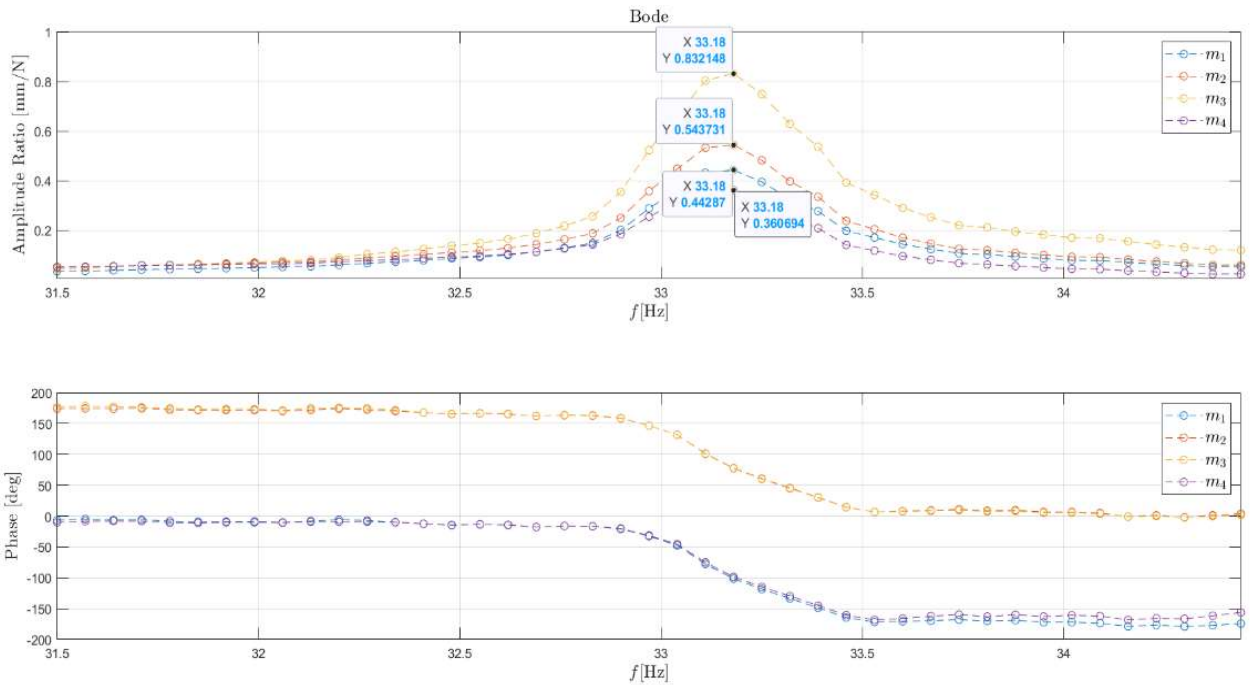


Figure 5: Bode diagram of frequency response of all masses around 33 [Hz], with steps of 0.07 [Hz]

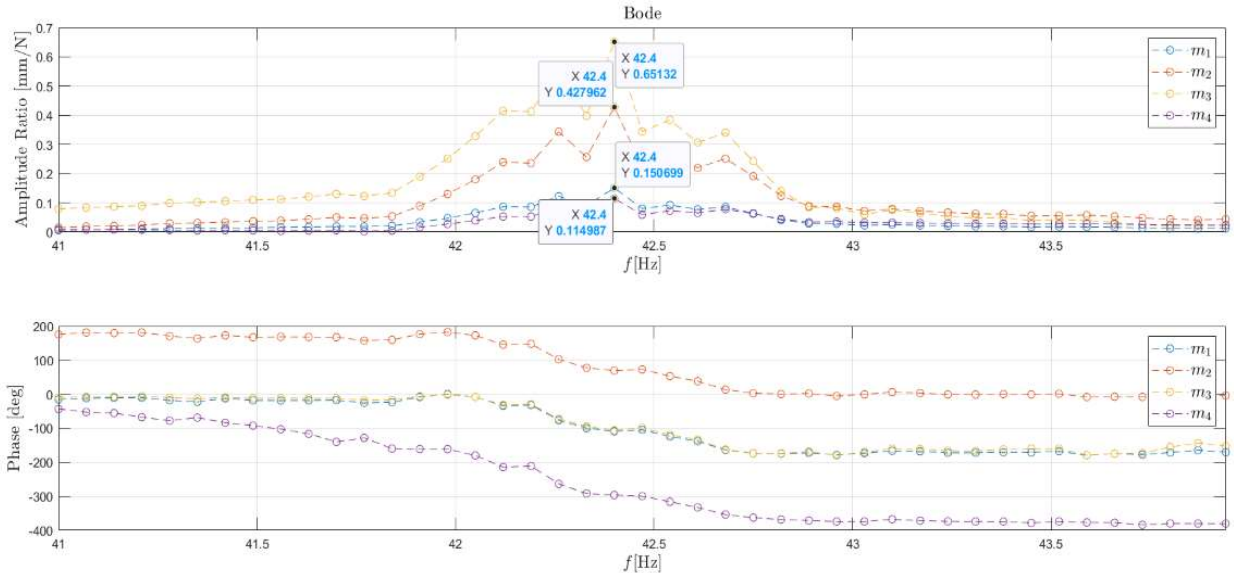


Figure 6: Bode diagram of frequency response of all masses around 42 [Hz], with steps of 0.07 [Hz]

In Figure 3, we get 2 peaks for every mass. We will therefore take the average value between these 2 peaks.

The results of this experiment can be seen in Table 1.

	$f_1 = 9.5 \text{ [Hz]}$	$f_2 = 19.5 \text{ [Hz]}$	$f_3 = 33 \text{ [Hz]}$	$f_4 = 42 \text{ [Hz]}$
Analytical	10.1559	19.587	32.57	41.689
Experimental	9.7	19.68	33.18	42.4
Error [%]	4.48 %	0.475 %	1.873 %	1.705 %

Table 1: Analytical vs experimental results

We get small errors between the analytical values and our experimental values. This can be due to external disturbances to the experimental system, which could introduce noise or fluctuations in the measured data. Another reason is that it is impossible to have a complete undamped system. There will always be some damping, which causes the experimented frequencies to be slightly lower than the theoretical undamped resonant frequency.

The following eigenvectors were obtained analytically:

$$\vec{v}_1 = \begin{bmatrix} -0.9129 \\ -0.9129 \\ -0.9129 \\ -0.9129 \end{bmatrix}; \vec{v}_2 = \begin{bmatrix} 1.1927 \\ 0.4940 \\ -0.4940 \\ -1.1927 \end{bmatrix}; \vec{v}_3 = \begin{bmatrix} 0.9129 \\ -0.9129 \\ -0.9129 \\ 0.9129 \end{bmatrix}; \vec{v}_4 = \begin{bmatrix} -0.4940 \\ 1.1927 \\ -1.1927 \\ 0.4940 \end{bmatrix}$$

We know that masses with a phase difference of 360° move in the same direction, and masses with a phase difference of 180° move in the opposite direction. This means that masses moving in the same direction should have the same sign in their eigenvector.

In Figure 3, we can see that all masses start at a phase of 0° , and after reaching the resonance frequency $f_1 = 9.7 \text{ [Hz]}$, move down to a phase of -180° . This corresponds with the eigenvector \vec{v}_1 , where all the signs are the same (negative). For Figure 4, Masses 1 & 2 move in the same phase, while Masses 3 & 4 move in the opposite phase. This corresponds to eigenvector \vec{v}_2 , where the first two values are positive, while the last two values are negative. For Figure 5, Masses 1 & 4 move in the same phase, while Masses 2 & 3 move in the opposite phase. This corresponds to eigenvector \vec{v}_3 , where the first & last value are positive, while the middle two values are negative. For Figure 6, we see Masses 1 & 3 move in the same phase, while Mass 2 moves in the opposite

phase. Mass 4 starts at 0° , but eventually reaches a difference of 360° between Mass 2, meaning they move in the same (opposite) phase. This can be due to measurement noise, as it can be seen in the bode graph that Mass 4 barely gets a peak. This corresponds to eigenvector \vec{v}_4 , where the first & third value are negative, while the second & fourth value are positive.

2.2 Nyquist plots analysis

The Nyquist plots around each of the 4 resonance frequencies with intervals of 0.07 [Hz] can be seen in the Figures below. The maximum amplitude for each mass has been marked. The results can be seen in the Tables below.

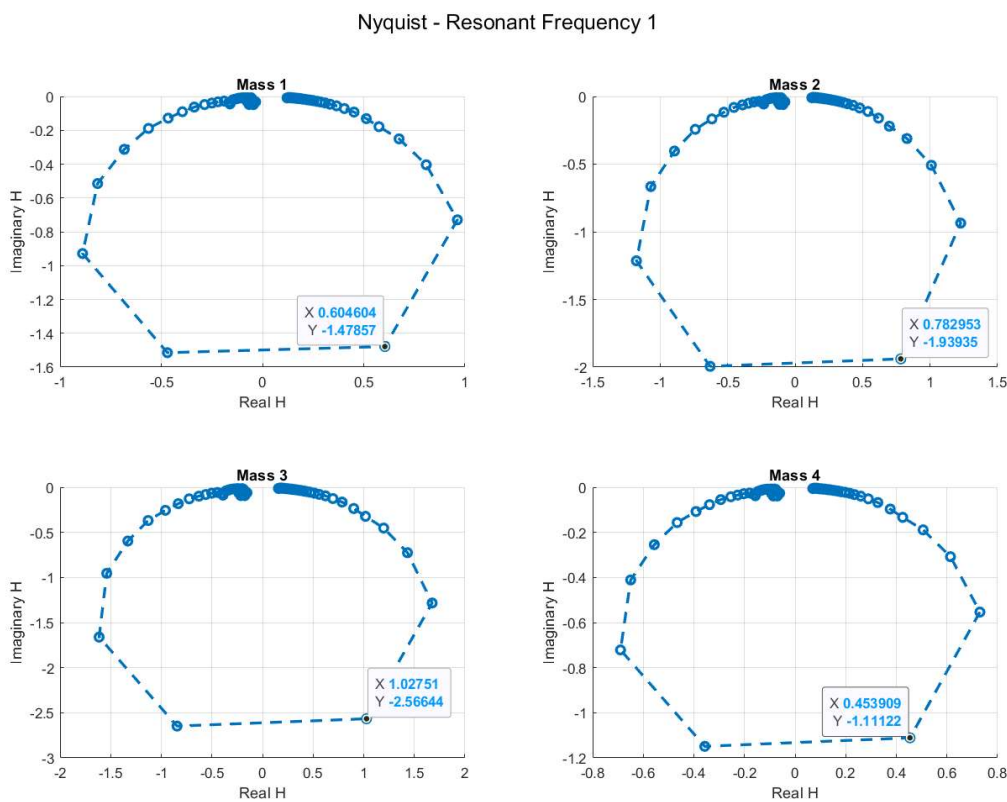


Figure 7: Nyquist plots around resonant frequency $f_1 = 9.5$ [Hz], with steps of 0.07 [Hz]

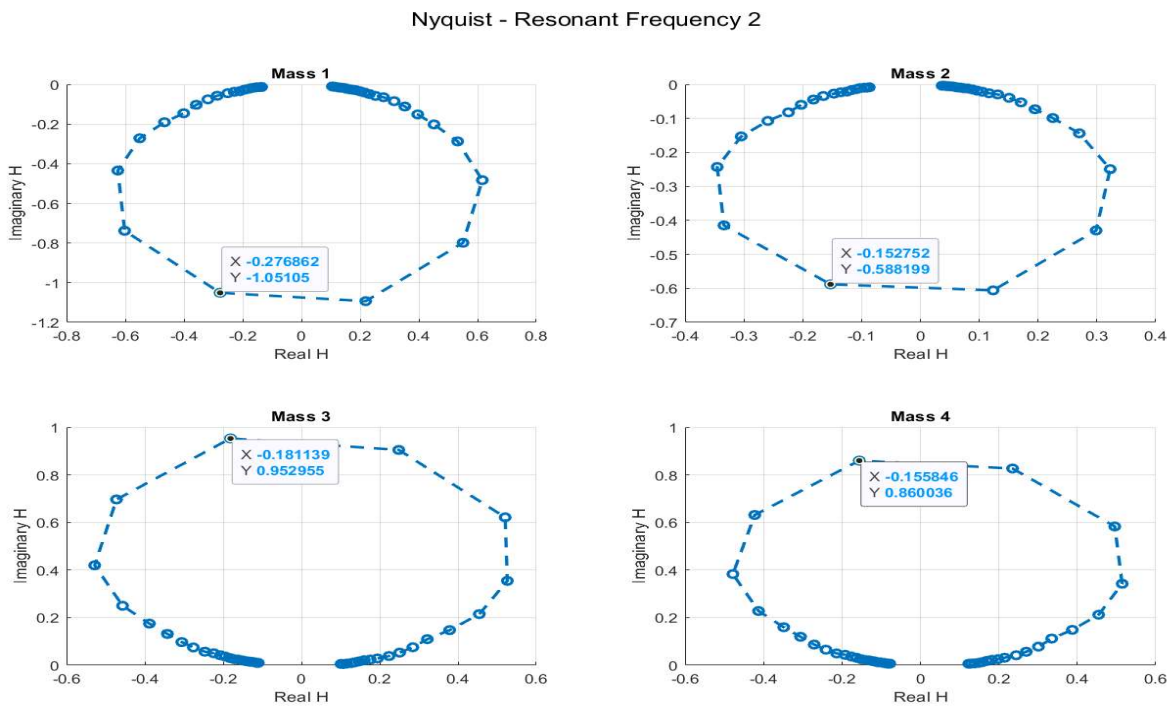


Figure 8: Nyquist plots around resonant frequency $f_1 = 19.5$ [Hz], with steps of 0.07 [Hz]

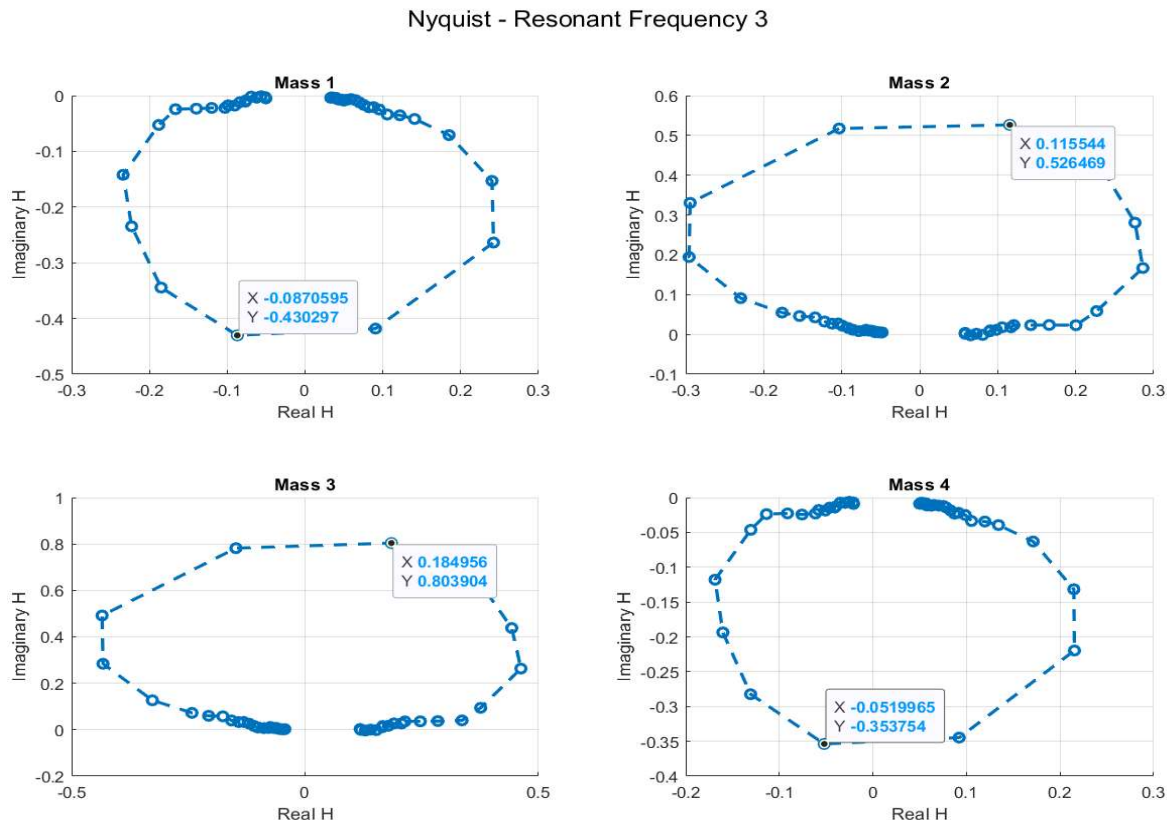


Figure 9: Nyquist plots around resonant frequency $f_1 = 33$ [Hz], with steps of 0.07 [Hz]

Nyquist - Resonant Frequency 4

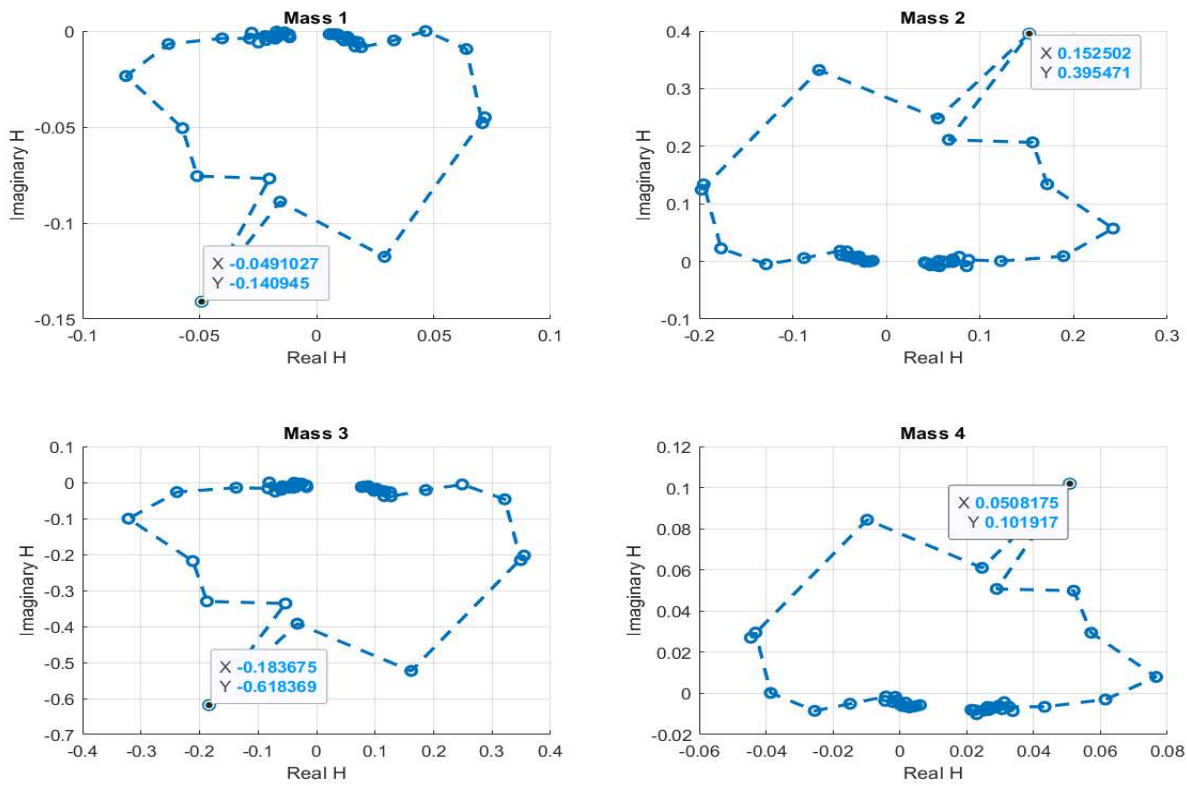


Figure 10: Nyquist plots around resonant frequency $f_1 = 42$ [Hz], with steps of 0.07 [Hz]

$f_1 = 9.5$	Mass 1	Mass 2	Mass 3	Mass 4
Complex	$0.6046 - 1.4786i$	$0.7829 - 1.9394i$	$1.0275 - 2.5664i$	$0.4539 - 1.1122i$
Phase [°]	-67.8°	-68.01°	-68.07°	-67.91°
Amplitude	1.5974	2.0912	2.7641	1.2012

Table 2: Nyquist plot analysis for $f_1 = 9.5$ [Hz]

$f_2 = 19.5$	Mass 1	Mass 2	Mass 3	Mass 4
Complex	$-0.2769 - 1.0511i$	$-0.1528 - 0.5882i$	$-0.1811 + 0.9529i$	$-0.1559 + 0.86i$
Phase [°]	-105.1°	-104.45°	100.75°	100.27°
Amplitude	1.0869	0.6076	0.9694	0.8730

Table 3: Nyquist plot analysis for $f_1 = 19.5$ [Hz]

	Mass 1	Mass 2	Mass 3	Mass 4
Complex	$-0.0871 - 0.4303i$	$0.1155 + 0.5265i$	$0.1849 + 0.8039i$	$-0.052 - 0.3538i$
Phase [°]	-101.26°	77.53°	77.47°	-98.34°
Amplitude	0.439	0.5391	0.8248	0.3575

Table 4: Nyquist plot analysis for $f_1 = 33$ [Hz]

$f_4 = 42$	Mass 1	Mass 2	Mass 3	Mass 4
Complex	$-0.0491 - 0.1409i$	$0.1525 + 0.3955i$	$-0.1836 - 0.6184i$	$0.0508 + 0.1019i$
Phase [°]	-109.49°	68.98°	-106.35°	63.59°
Amplitude	0.149	0.4239	0.6445	0.114

Table 5: Nyquist plot analysis for $f_1 = 42$ [Hz]

We can see that the amplitudes of the masses for the 4 resonant frequencies are similar to the ones seen on the Bode plots. We can also see that for f_1 and f_4 , the phases have the same sign as the corresponding eigenvectors \vec{v}_1 and \vec{v}_4 . For f_2 and f_3 , the sign of the phases of the maximum amplitude are opposite that of the corresponding eigenvectors \vec{v}_2 and \vec{v}_3 , but the combinations of signs corresponds to the combination of the eigenvectors sign, meaning the masses with the same sign move together.

3. Damping effect investigation using Q-factor

To see the effect of damping on the masses, we conducted the first experiment again, only this time increasing the damping by approaching the magnets to a distance of 0.1 [mm] from the masses. The bode plots around the first natural frequency, for both damping values, can be seen in Figures 11 & 12.

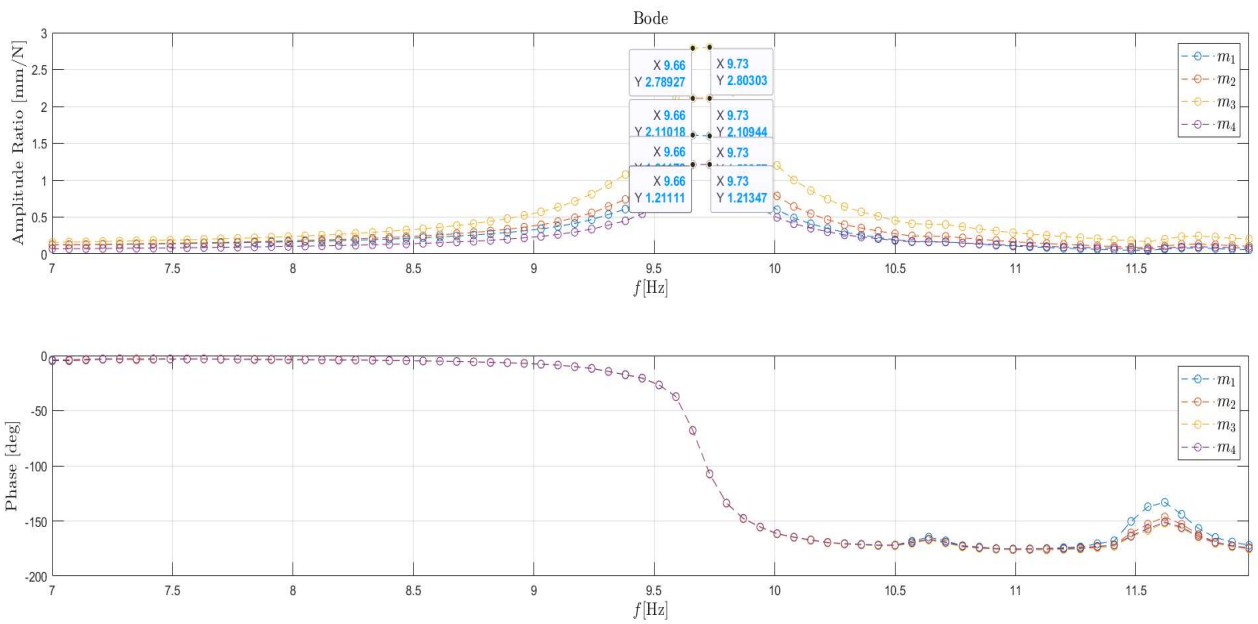


Figure 11: Bode diagram of frequency response of all masses around 9.5 [Hz], with steps of 0.07 [Hz], low damping

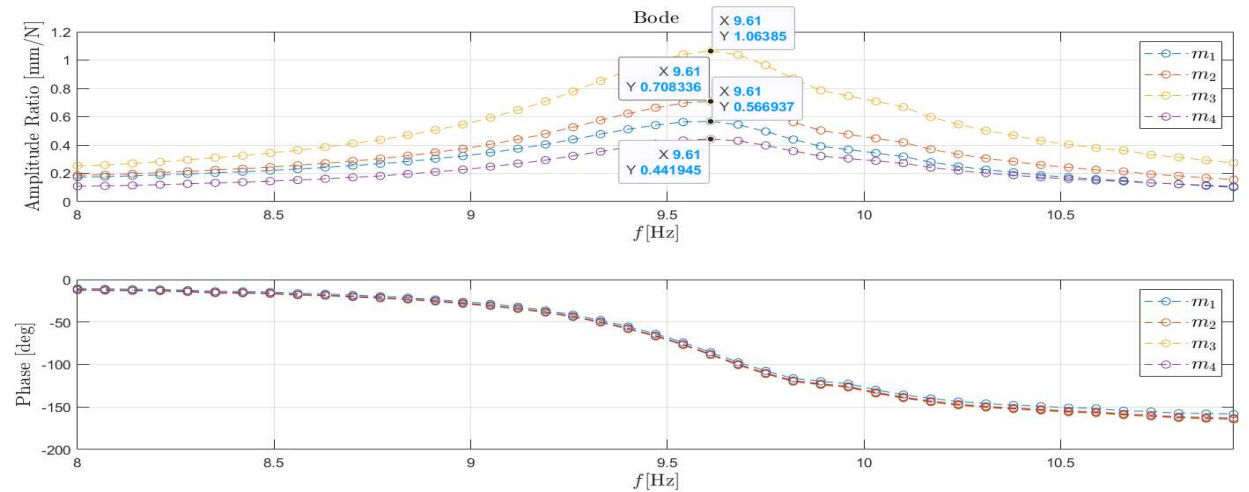


Figure 12: Bode diagram of frequency response of all masses around 9.5 [Hz], with steps of 0.07 [Hz], high damping

To calculate the Q-factor, we need to find the width of each frequency, at a height of $\frac{1}{\sqrt{2}}$ of the resonance frequency. This was done using the MATLAB figures. The results can be seen in the following table.

LOW DAMPING	f_n	$A(f_n)$	$\frac{1}{\sqrt{2}}A(f_n)$	Δf	$Q = \frac{f_n}{\Delta f}$	$\zeta = \frac{1}{2Q}$
Mass 1	9.7	2.803	1.982	$9.87 - 9.59 = 0.28$	34.6429	0.01443
Mass 2	9.7	2.109	1.4913	$9.87 - 9.59 = 0.28$	34.6429	0.01443
Mass 3	9.7	1.599	1.1306	$9.87 - 9.59 = 0.28$	34.6429	0.01443
Mass 4	9.7	1.2135	0.858	$9.87 - 9.59 = 0.28$	34.6429	0.01443

Table 6: Damping ratio for low damping results

HIGH DAMPING	f_n	$A(f_n)$	$\frac{1}{\sqrt{2}}A(f_n)$	Δf	$Q = \frac{f_n}{\Delta f}$	$\zeta = \frac{1}{2Q}$
Mass 1	9.61	1.06385	0.75226	$9.96 - 9.26 = 0.7$	13.7286	0.03642
Mass 2	9.61	0.708336	0.50087	$9.89 - 9.19 = 0.7$	13.7286	0.03642
Mass 3	9.61	0.566937	0.400885	$9.89 - 9.19 = 0.7$	13.7286	0.03642
Mass 4	9.61	0.441945	0.3125	$9.89 - 9.26 = 0.63$	15.2539	0.03278

Table 7: Damping ratio for high damping results

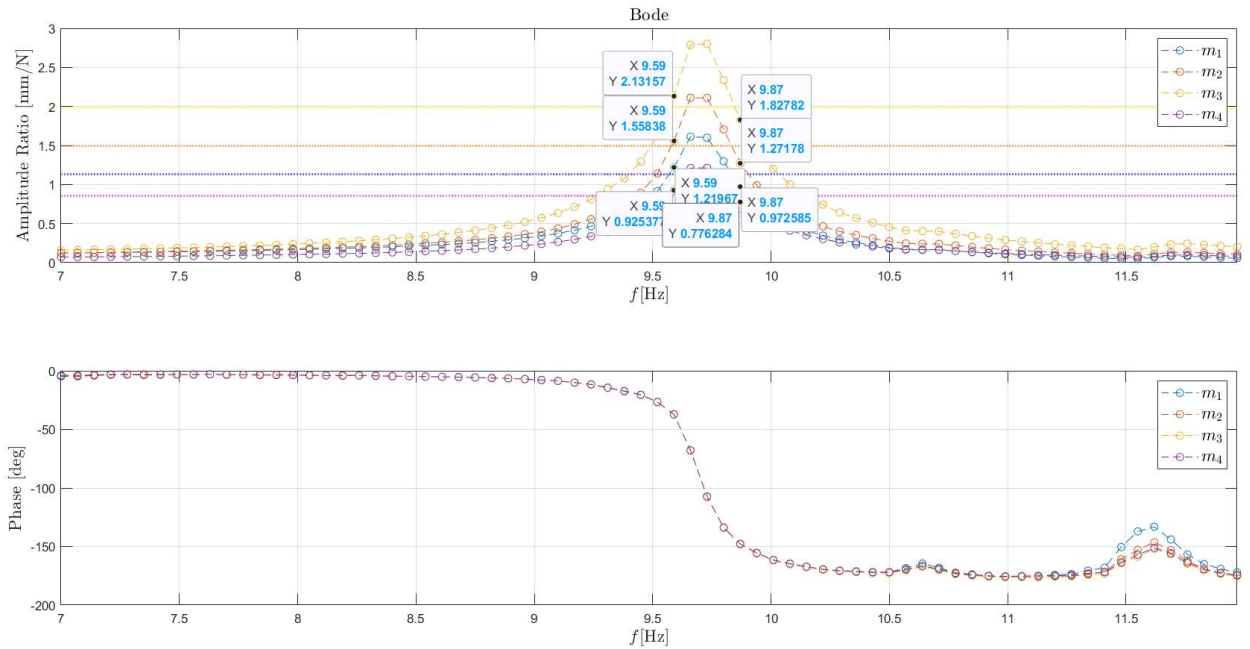


Figure 13: Bode graph for Q-factor calculation, low damping

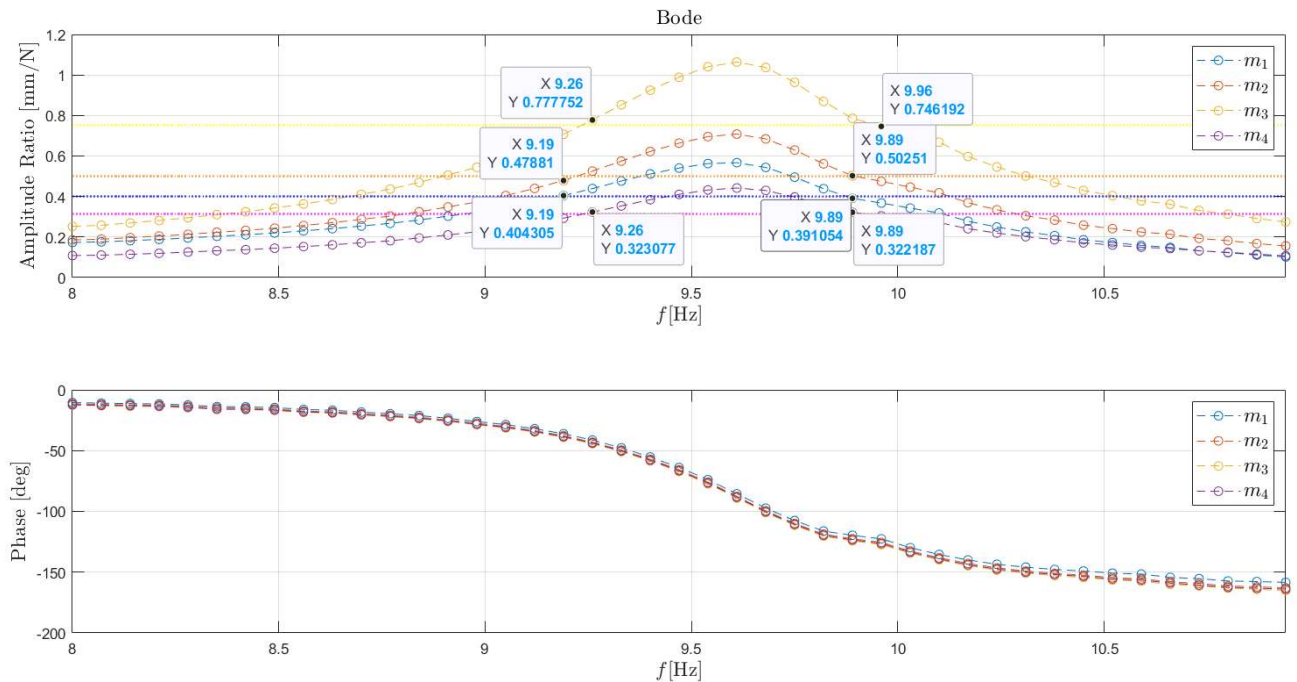


Figure 14: Bode graph for Q-factor calculation, high damping

Let's look at the effect on the natural frequencies, affected by the damping ratio with the formula $f_d = f_N \sqrt{1 - \zeta^2}$. For low damping, our resonance frequency is $f_d = 9.7$, the theoretical natural frequency is $f_N = 10.1559$, and our damping ratio is $\zeta = 0.01443$. Plugging these values into the formula, we get $f_d = 10.15484$, which has an error of 4.689 %. For high damping, our resonance frequency is $f_d = 9.61$, and our damping ratio is $\zeta = 0.03642$. Plugging in these values, we get $f_d = 10.14916$, which has an error of 5.61 %. On both cases, the theoretical natural frequency is higher. This is normal, as damped systems always reduces the resonance frequency. The resonance frequency of the higher damped system is shifted more than that of low damping. The differences and errors suggest that there are additional damping effects, or that there are experimental errors in our observance of the width. We can see on Figures 13 & 14 that the values chosen are not exactly on a height of $1/\sqrt{2}$, because we do not have fine results around the peak. This can be improved if we take finer steps around the natural frequency.

4. Decay envelope measurement

The damping ratio can also be calculated using the decay envelope at the natural frequency f_N . A sinusoidal excitation at the first natural frequency $f_{N1} = 10.1559$ [Hz] has been applied, with enough time to bring the system to a steady state. Then, we do a sudden stop to the excitation. The decay has been measured using an LS fit of the form $a + b \exp(ct) * \cos(dt + e)$. Then, using the parameters of the fit, we get an approximation of the decay with the exponential function of the form $A_0 \exp(-t/\tau)$. The damping ratio can be calculated with $\zeta = (2\pi f_N \tau)^{-1}$. We will do this for all 4 masses. The results can be seen in the Figures & the table below.

4.1 Low damping

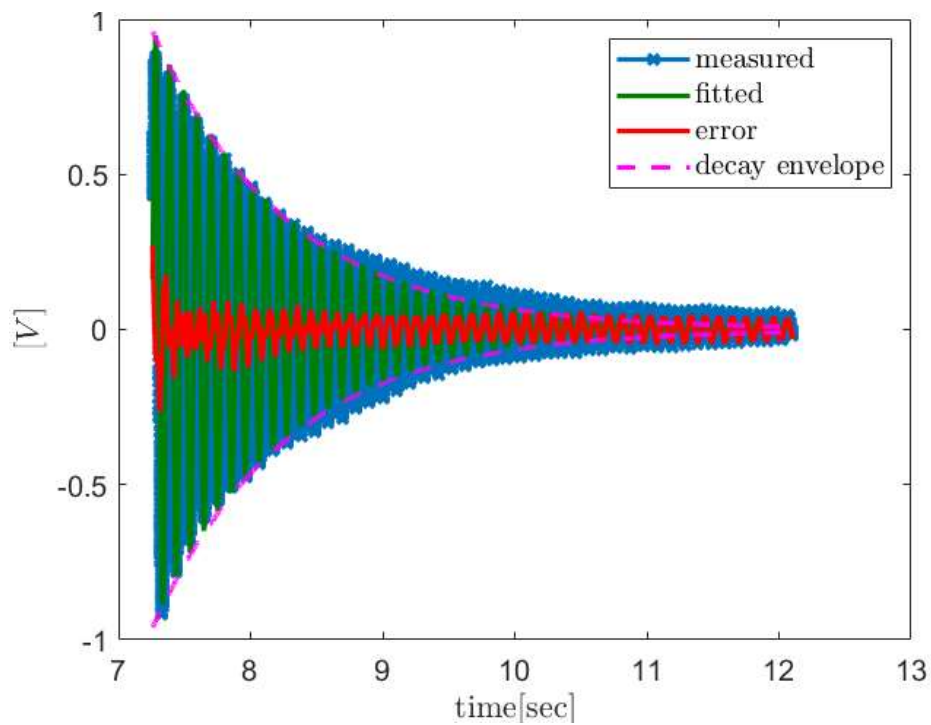


Figure 15: Decay envelope at the first natural frequency of Mass 1

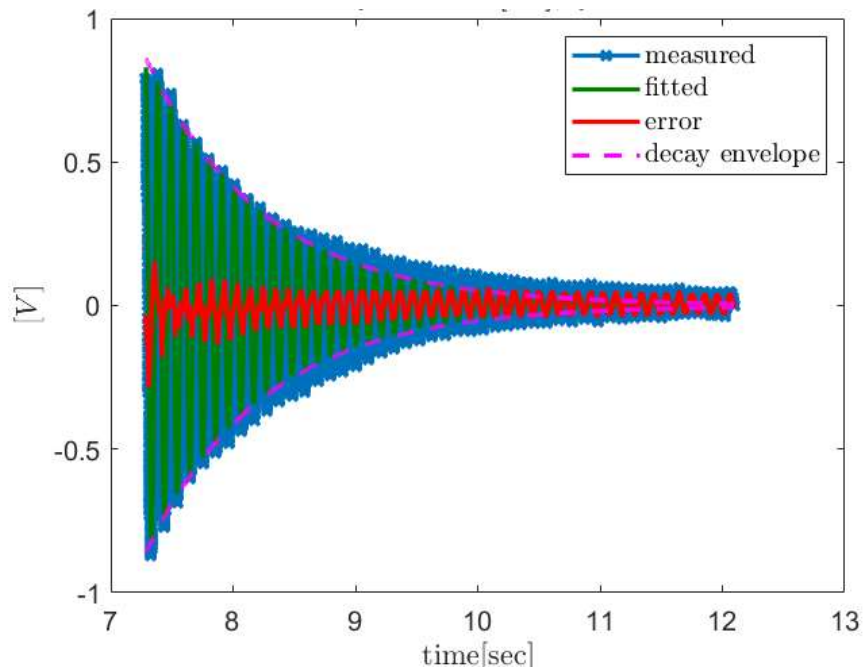


Figure 16: Decay envelope at the first natural frequency of Mass 2

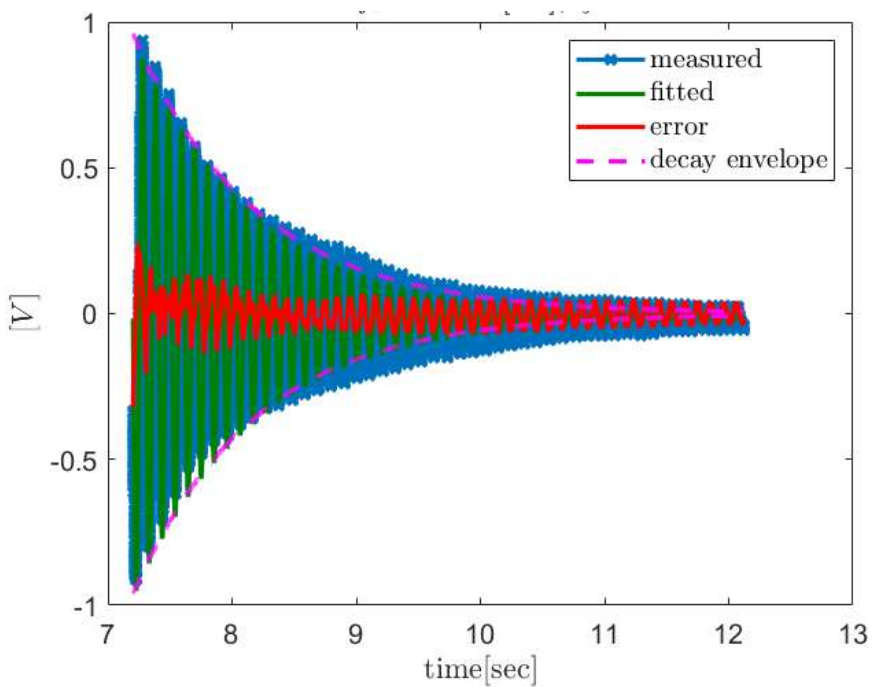


Figure 17: Decay envelope at the first natural frequency of Mass 3

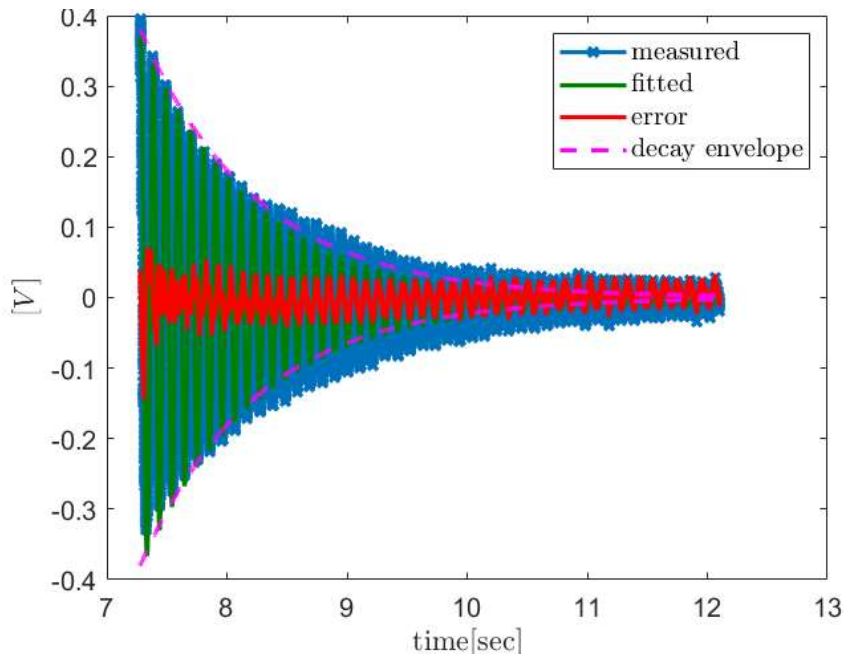


Figure 18: Decay envelope at the first natural frequency of Mass 4

LOW DAMPING	f_{N1}	A_0	τ	R^2 of fit	ζ_{decay}	$\zeta_{Q-factor}$	Error %
Mass 1	10.1559	455.612	1.1659	0.9726	0.01344	0.01443	6.86
Mass 2	10.1559	-1354.1362	0.9734	0.9646	0.0161	0.01443	11.573
Mass 3	10.1559	-1857.0471	0.9508	0.951	0.01648	0.01443	14.207
Mass 4	10.1559	-691.8175	0.9562	0.9562	0.016389	0.01443	13.5758

Table 8: Results of decay function for low damping

We can see that there is a relatively large error between the different damping ratios. This might be due to the exponential function being on the fitted curve, and not on the measured data. Other reasons can be that the decay parameters were incorrectly picked, not giving us a good fit, and therefore a bad exponential function. This can be seen as the R^2 of the fit and the Error have similarities. When the R^2 value decreases, the error increases.

4.2 High damping

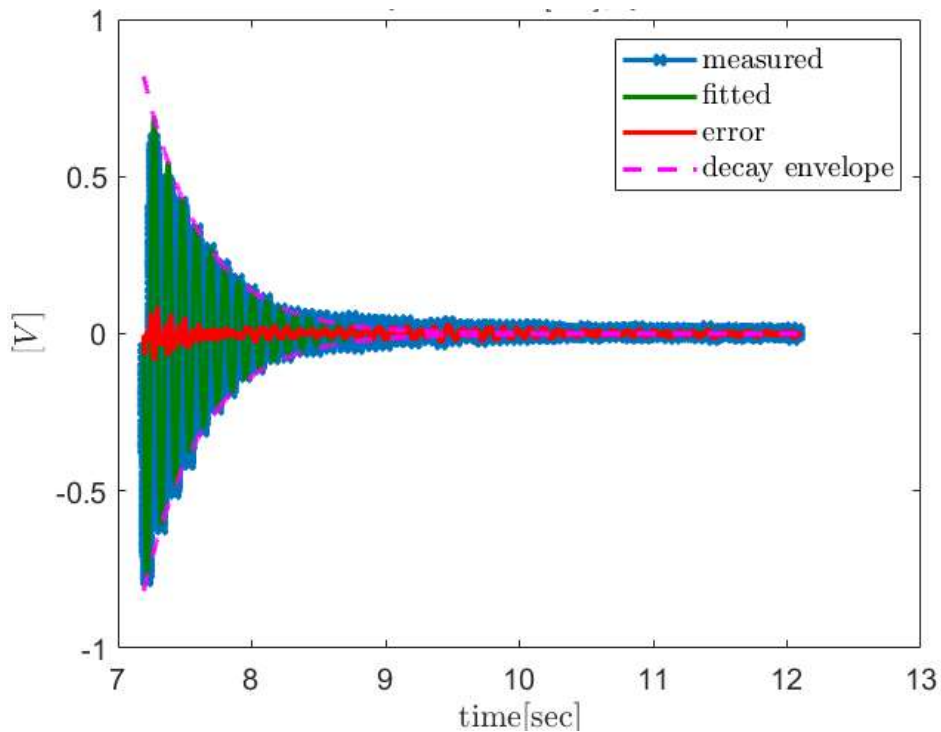


Figure 19: Decay envelope at the first natural frequency of Mass 1

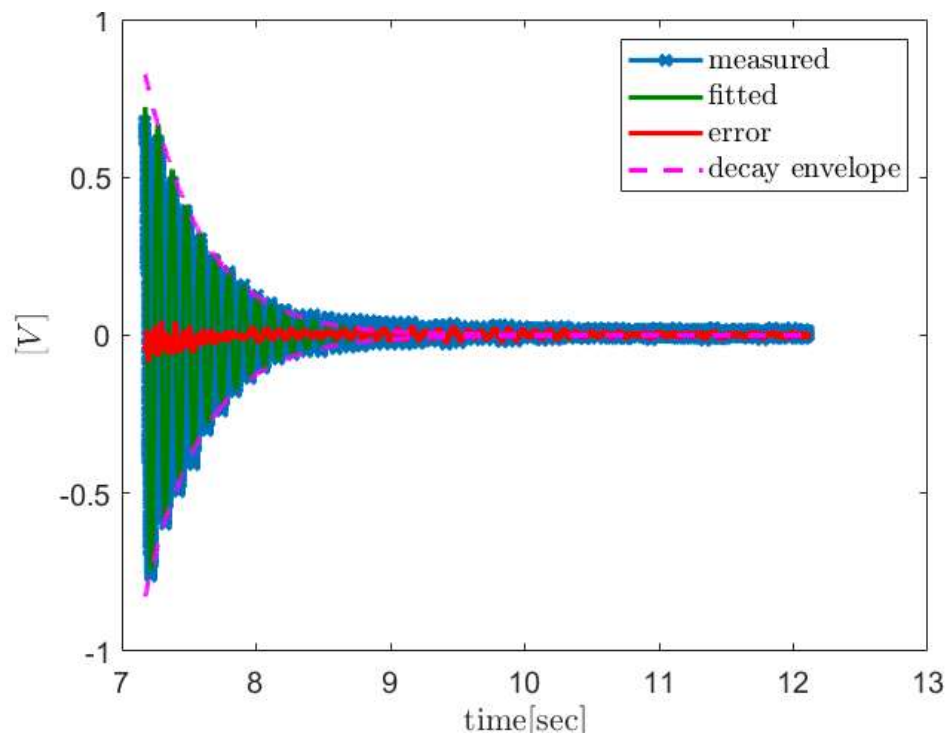


Figure 20: Decay envelope at the first natural frequency of Mass 2

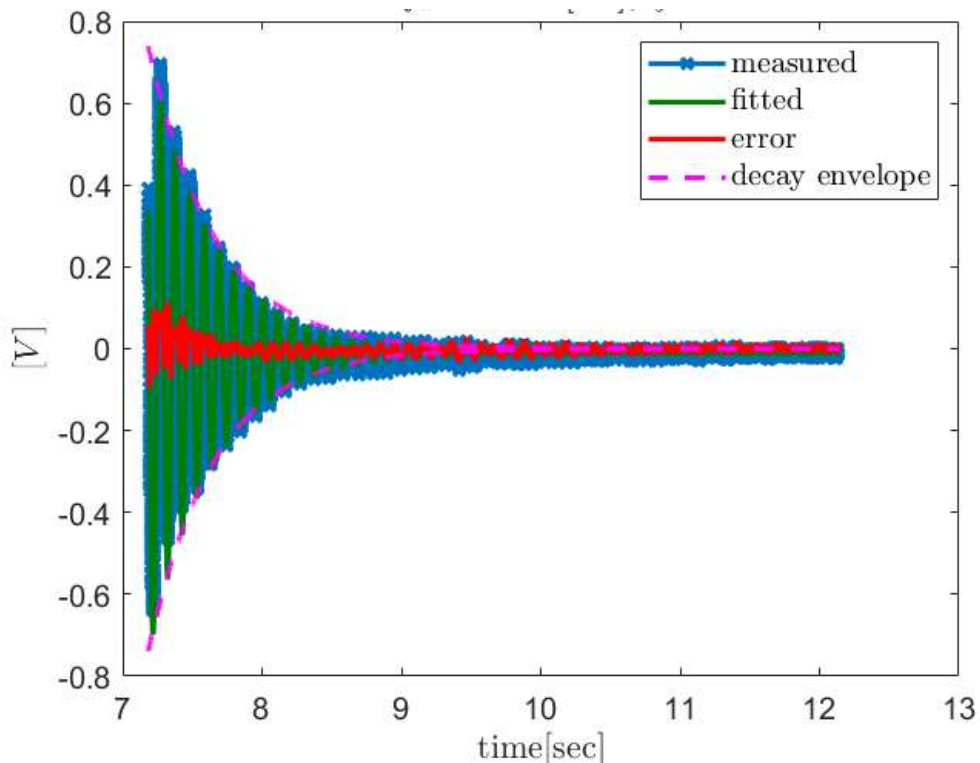


Figure 21: Decay envelope at the first natural frequency of Mass 3

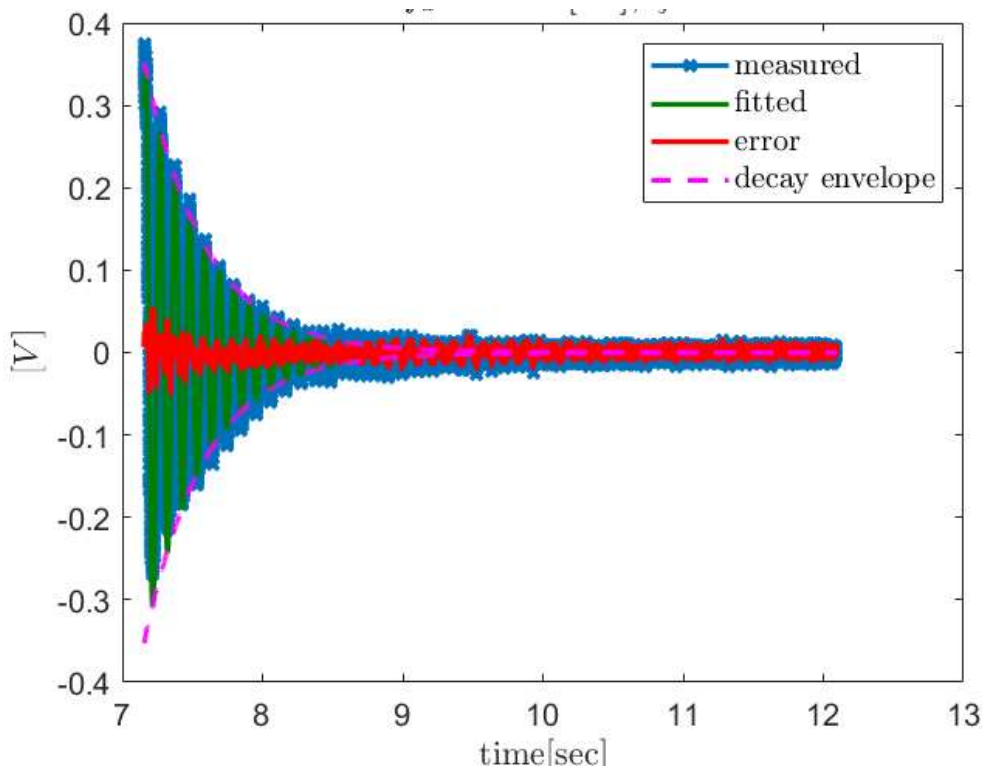


Figure 22: Decay envelope at the first natural frequency of Mass 4

HIGH DAMPING	f_{N1}	A_0	τ	R^2 of fit	ζ_{decay}	$\zeta_{Q-factor}$	Error %
Mass 1	10.1559	-7273064.46	0.4496	0.9899	0.03486	0.03642	4.283
Mass 2	10.1559	-11549209.66	0.4361	0.9895	0.03594	0.03642	1.318
Mass 3	10.1559	-2469585.54	0.4782	0.9799	0.03277	0.03642	10.022
Mass 4	10.1559	-4905843.97	0.435	0.9797	0.03603	0.03278	9.915

Table 9: Results of decay function for high damping

We can see that for high damping, the error between the damping ratios for the two methods is slightly smaller than with low damping. This might be due to having an overall better fit, as the R^2 of the fit are slightly higher than those with low damping.

5. Summary

In this lab, we conducted several experiments to investigate the dynamic response of an oscillatory system, focusing on frequency response, damping effects, and damping ratio calculations. The main conclusions for each experiment are given below.

5.1 Frequency response

We generated Bode plots and Nyquist plots to characterize the system's frequency response. The analytical and experimental values of the resonant frequencies were compared, showing small errors due to external disturbances and inherent system damping.

5.2 Damping effect investigation using Q-factor

We calculated the Q-factor and observed how the damping ratio affected the natural frequencies. The theoretical models predicted a slight shift in the natural frequencies due to damping, which was consistent with our experimental observations. However, the errors in the damping ratios, particularly for low damping, were slightly larger due to the sensitivity of the measurement methods to noise and disturbances. This error can be reduced by taking finer steps in our measurement, and having minimal disturbances that can affect the system.

5.3 Decay Envelope Measurement

The decay envelope method provided an alternative way to calculate the damping ratio. The comparison of damping ratios from the Q-factor and decay envelope methods showed discrepancies, particularly for low damping. This was attributed to noise and the precision of the exponential fit. As the exponential curve was applied on the fit, and not directly on the measurements. We can improve this by having more accurate measurements and choosing an overall better fit parameters with a higher accuracy (higher R^2 value).